



Review

# Fentanyl Structure as a Scaffold for Opioid/Non-Opioid Multitarget Analgesics

Piotr F. J. Lipiński \* and Joanna Matalińska

Department of Neuropeptides, Mossakowski Medical Research Institute Polish Academy of Sciences, Pawińskiego 5, 02-106 Warsaw, Poland; jmatalinska@imdik.pan.pl

\* Correspondence: plipinski@imdik.pan.pl

**Abstract:** One of the strategies in the search for safe and effective analgesic drugs is the design of multitarget analgesics. Such compounds are intended to have high affinity and activity at more than one molecular target involved in pain modulation. In the present contribution we summarize the attempts in which fentanyl or its substructures were used as a  $\mu$ -opioid receptor pharmacophoric fragment and a scaffold to which fragments related to non-opioid receptors were attached. The non-opioid 'second' targets included proteins as diverse as imidazoline I<sub>2</sub> binding sites, CB<sub>1</sub> cannabinoid receptor, NK<sub>1</sub> tachykinin receptor, D<sub>2</sub> dopamine receptor, cyclooxygenases, fatty acid amide hydrolase and monoacylglycerol lipase and  $\sigma$ <sub>1</sub> receptor. Reviewing the individual attempts, we outline the chemistry, the obtained pharmacological properties and structure-activity relationships. Finally, we discuss the possible directions for future work.

**Keywords:** fentanyl; heterodimers; multitarget drugs; pain; structure-activity relationships



**Citation:** Lipiński, P.F.J.; Matalińska, J. Fentanyl Structure as a Scaffold for Opioid/Non-Opioid Multitarget Analgesics. *Int. J. Mol. Sci.* **2022**, *23*, 2766. <https://doi.org/10.3390/ijms23052766>

Academic Editors: Renato B. Pereira and David M. Pereira

Received: 11 February 2022

Accepted: 1 March 2022

Published: 2 March 2022

**Publisher's Note:** MDPI stays neutral with regard to jurisdictional claims in published maps and institutional affiliations.



**Copyright:** © 2022 by the authors. Licensee MDPI, Basel, Switzerland. This article is an open access article distributed under the terms and conditions of the Creative Commons Attribution (CC BY) license (<https://creativecommons.org/licenses/by/4.0/>).

## 1. Introduction

Finding novel drugs for effective and safe management of severe and/or chronic pain poses a major challenge for modern medicinal chemistry and pharmacology. The key element of our current therapeutical toolbox against pain are agonists of the  $\mu$ -opioid receptor (MOR). These, while being highly effective in severe acute conditions, are not devoid of adverse effects that turn out most problematic with prolonged use. Many patients taking opioids suffer from sedation, nausea, hard-to-treat constipations, paradoxical hyperalgesia or endocrinologic dysfunctions [1,2]. Long-term opioid use increases the risk of developing physical dependence and addiction [1]. Tolerance to opioid analgesia (but not to the opioid side effects) appears relatively quickly [3], requiring escalation of the dosage, but this in turn exacerbates the mentioned side effects. Moreover, the use of classical opioids in neuropathic pain conditions is often of limited effectiveness [4].

Several strategies have been devised with the hope of achieving effective opioid analgesia with improved side effects profile [5]. One that over the years has enjoyed a good deal of interest from the researchers is the development of multitarget analgesic (MTA) compounds [6,7]. Substances of this type have significant affinity and activity at more than one molecular target involved in pain modulation. Among MTAs one can distinguish multifunctional and multivalent compounds (Figure 1A) [7]. Multivalent (usually bivalent) compounds are able to bind to a few molecular targets at the very same time, for example by targeting heterodimers formed by opioid receptors with other receptors [8]. On the contrary, multifunctional (usually bifunctional, dual) compounds possess high affinity to more than one target but bind to each of these in separate.

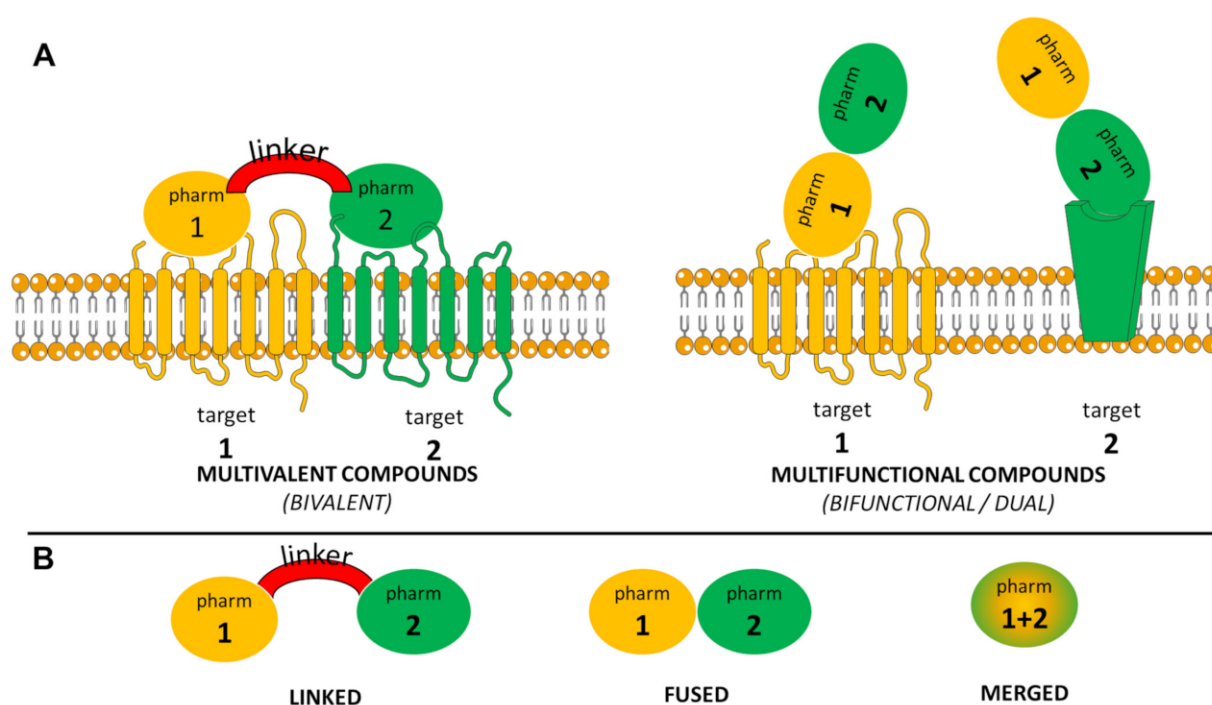


**Figure 1.** (A) Schematic distinction between multivalent and multifunctional compounds. (B) Schematic representation of various types of multitarget compounds according to the degree to which the included pharmacophores are integrated. ‘Pharm’ stands for ‘pharmacophore’.

That a multitarget pharmacological profile could be therapeutically beneficial for analgesics arises from the complex nature of many pain conditions which involves interplay between numerous signalling pathways. The interplay between pro- and antinociceptive factors is also thought to be responsible for analgesic tolerance, hyperalgesia, and low efficacy of opioids in neuropathic pain [9]. By simultaneous targeting of MOR and an additional receptor, a multifunctional analgesic could counteract the side effects directly or indirectly, in the latter case by improving efficacy and thus lowering the need for the activation of opioid pathways. Additional signalling components are also sometimes expected to provide satisfactory activity in neuropathic pain.

In the search for MTAs, compounds targeting many diverse pairs of molecular targets have been obtained [6]. The usual ‘major’ target in these pairs is the  $\mu$ -opioid receptor (MOR). The auxiliary targets may be other G-protein coupled receptors (GPCRs), e.g., CB<sub>1</sub> cannabinoid receptor [10,11], NK<sub>1</sub> tachykinin receptor [12,13], D<sub>2</sub> dopamine receptor, CCK<sub>2</sub> cholecystikinin receptor [14,15], neurotensin receptor [16,17], MC<sub>4</sub> melanocortin receptor [18,19], neuropeptide FF receptor [20] or  $\alpha_2$ -adrenergic receptor [21]. The second target could be also a non-GPCR receptor ( $\sigma_1$  receptors [22]), an enzyme (cyclooxygenases [23], fatty acid amide hydrolase and monoacylglycerol lipase [24]), an ion channel (voltage gated calcium channels [25]) or a binding site of a less clear character (imidazoline I<sub>2</sub> binding sites [26–28]). Moreover, a separate and a well-developed subfield are MTAs aimed at targeting of two or more different opioid receptor subtypes [7].

MTAs (or multitarget drugs in general) are designed by combining pharmacophores of the two (or more) desired molecular targets. Depending on the degree to which the structural elements of both pharmacophores are integrated, one can speak of ‘linked’, ‘fused’ or ‘merged’ dual ligands (Figure 1B) [29,30]. In the ‘linked’ ligands, the structural fragments related to the individual targets are joined by a linker/spacer (sometimes a very long one). In the ‘fused’ molecules, the fragments are directly combined, and no spacer can be discerned. In the ‘merged’ ligands, there is an at least partial overlap of the pharmacophoric elements.

Whichever approach one is going to follow in their search for MTAs, a key issue is the choice of the pharmacophoric fragments to be used. In the present contribution, we shall summarize the attempts to create MTAs that (directly or indirectly) utilized fentanyl (1.1, Figure 2) or its substructures as a  $\mu$ -opioid pharmacophore and a scaffold to append (or to melt into) pharmacophoric elements of other, non-opioid molecular targets.

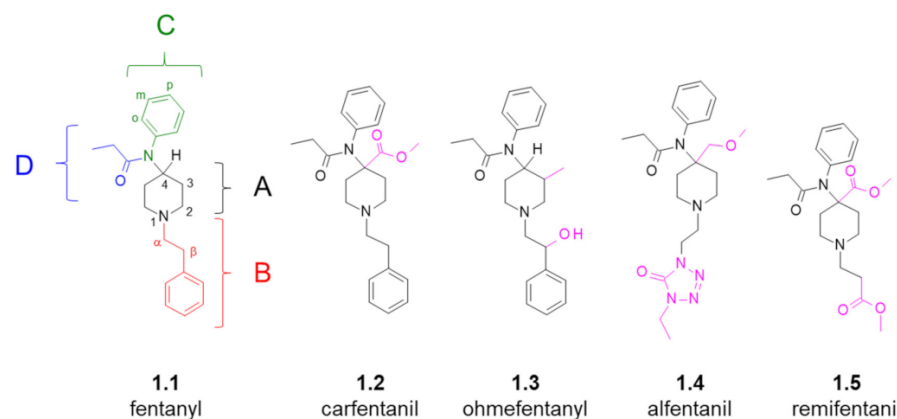
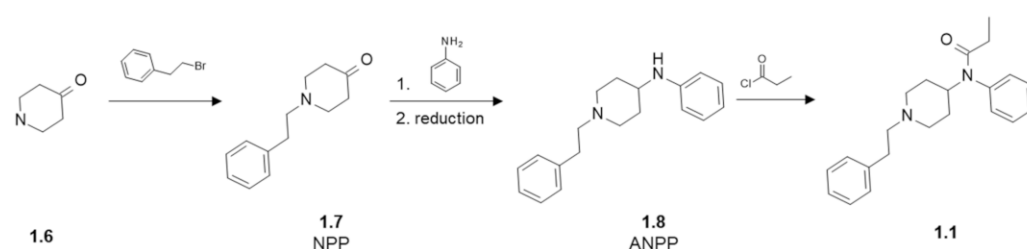


**Figure 2.** Structure of fentanyl (with its logical dissection and position numbering convention shown) and of a few important analogues thereof. Modifications (compared to the parent compound) are marked in pink.

Fentanyl (*N*-phenyl-*N*-[1-(2-phenylethyl)piperidin-4-yl]propanamide, 1.1) is a very useful and a well-established analgesic and anaesthetic drug [31]. The compound has high affinity for MOR and displays potent agonistic properties at this receptor. It is also very lipophilic and thanks to this it readily distributes into the central nervous system (CNS), rapidly producing the opioid effect. Depending on the particular testing conditions, fentanyl may be 50 to 100 times more potent an analgesic than morphine [32]. In clinical settings (in low doses, with short-term use), fentanyl is rather safe, although illicit recreational use is associated with thousands of ‘fentanyl deaths’ each year [33].

The synthesis of fentanyl and of many basic analogues can be conveniently accomplished in three steps (Scheme 1) as demonstrated by an optimized method of Valdez et al. [34]. In Step I, piperidin-4-one (1.6) is *N*-alkylated with e.g., 2-phenethyl bromide. In Step II, the resulting *N*-phenethylpiperidin-4-one (NPP, 1.7) is subject to reductive amination with aniline to yield (via a Schiff base) 4-anilino *N*-phenethyl-piperidine (ANPP, 1.8). Finally, the amine 1.8 is acylated using e.g., propionyl chloride. Alterations of the alkylating agents, amines or the acylating agents provide access to many fentanyl analogues, while leaving this basic synthetic scheme untouched. The original fentanyl syntheses [35,36] as well as syntheses found in many other papers for other analogues tend to utilize *N*-protected piperidin-4-ones, which are deprotected and *N*-alkylated only after other desired elements have been introduced.



**Scheme 1.** Exemplary synthetic route to fentanyl. Many basic analogues can be accessed by modifications of the alkylating agent, amine or acylating agent. NPP—*N*-phenethylpiperidin-4-one. ANPP—4-anilino *N*-phenethyl-piperidine.

In terms of structure (Figure 2), the core of fentanyl is the piperidine ring (region A). In position 1, this ring is decorated with the phenethyl group (region B), while attached in position 4 is a nitrogen atom substituted with a phenyl ring (region C) and a propionyl group (region D). Over the years, this elementary structure has been thoroughly explored and numerous analogues of fentanyl (“fentanyls” or “fentalogues”) were synthesized for probing SAR of the 4-anilidopiperidine class of analgesics. A recent concise SAR and chemistry summary was provided by Vardanyan and Hruby [37]. Here, let us mention only that the following modifications/substitutions could be found in the most potent derivatives:

(region A): 4-carboxymethyl, 4-methoxymethyl, 3-methyl,

(region B):  $\alpha$ -methyl,  $\beta$ -hydroxyl (if accompanied by 3-methyl in the region A), replacement of the phenyl ring for heterocyclic aromatics,

(region C): *p*-fluoro substitution at the ring (some other substitutions and replacements could be tolerated or beneficial, too).

(region D): alicyclic fragments (e.g., cyclopropyl), linear (elongated) or branched alkyl chains, ether fragments, aromatic fragments (e.g., 2-furanyl).

Particularly worth pinpointing seem such interesting analogues as ultrapotent  $\mu$ OR agonists, such as carfentanil (1.2, [38]) or ohmefentanil (1.3, [39]), and ultrashort acting analgesics, such as alfentanil (1.4, [40]) or remifentanil (1.5, [41]).

That the structure of fentanyl (1.1) may be a good starting point for creating MTAs derives from (1) its pharmacological properties, (2) a relatively facile chemistry by which diverse analogues and functionalized derivatives can be accessed, (3) wealth of available structure-activity relationships (SAR) data.

## 2. Fentanyl-Based MTAs Targeting MOR and I<sub>2</sub>-Imidazoline Binding Sites

Historically, the first attempt to utilize the fentanyl scaffold for creating multitarget opioid/non-opioid compounds was the one in which researchers tried to obtain dual ligands for MOR and I<sub>2</sub>-imidazoline binding sites (I<sub>2</sub>-IBS) [26–28].

Both the nature and the role of I<sub>2</sub>-IBS has remained elusive. According to Regunathan and Reis [42], I<sub>2</sub> imidazoline binding sites (receptors) are nonadrenergic binding sites that have high affinity for [<sup>3</sup>H]-idazoxan (2.1, Figure 3A) and a substantially lower affinity for [<sup>3</sup>H]-clonidine (2.2) or [<sup>3</sup>H]-*para*-aminoclonidine. Rather than being a single protein, I<sub>2</sub>-IBS seem to represent a heterogenous population of binding sites [43]. Their identity is still not conclusively established. In 2009, a brain creatine kinase (B-CK) was found to be an I<sub>2</sub> imidazoline binding protein [44], but several other I<sub>2</sub>-binding sites were immunodetected and some are suspected to be allosteric binding sites on monoamine oxidases A and B [43].

From the standpoint of pharmacology, I<sub>2</sub>-IBS ligands are considered for their neuroprotective actions and for their antinociceptive effects in some models of chronic and neuropathic pain [45,46]. So far, no approved drug has been developed based on imidazoline receptor concept, but an I<sub>2</sub>-IBS agonist CR4056 has some chance of becoming one, since recently it has successfully passed the Phase 2 clinical trial for chronic pain associated with osteoarthritis [47].

Apart from their analgesic action as single agents, I<sub>2</sub>-imidazoline agonists may be adjuvants to opioids. Simultaneous administration of both had been shown to produce synergistic antinociceptive effect and to attenuate tolerance to opioid action [45,46]. Based on this, a Spanish group proposed that development of hybrid molecules binding to both MOR and I<sub>2</sub>-IBS might be an interesting strategy for finding novel analgesic compounds with improved properties [26–28]. They presented fentanyl derivatives designed to have affinity for both these targets.

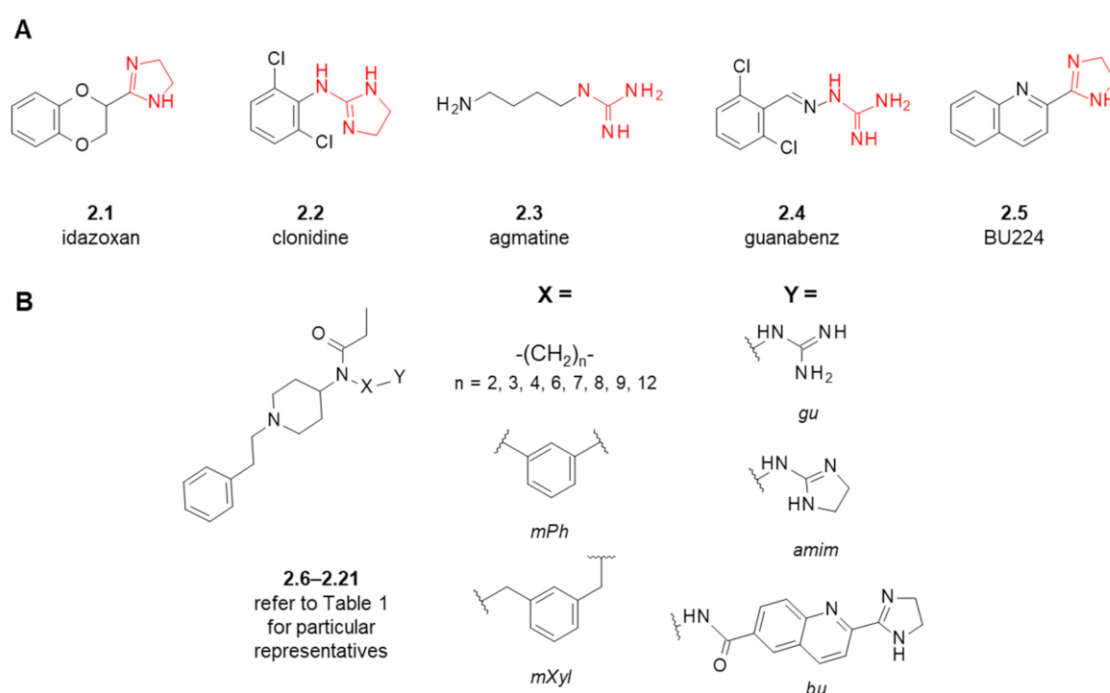
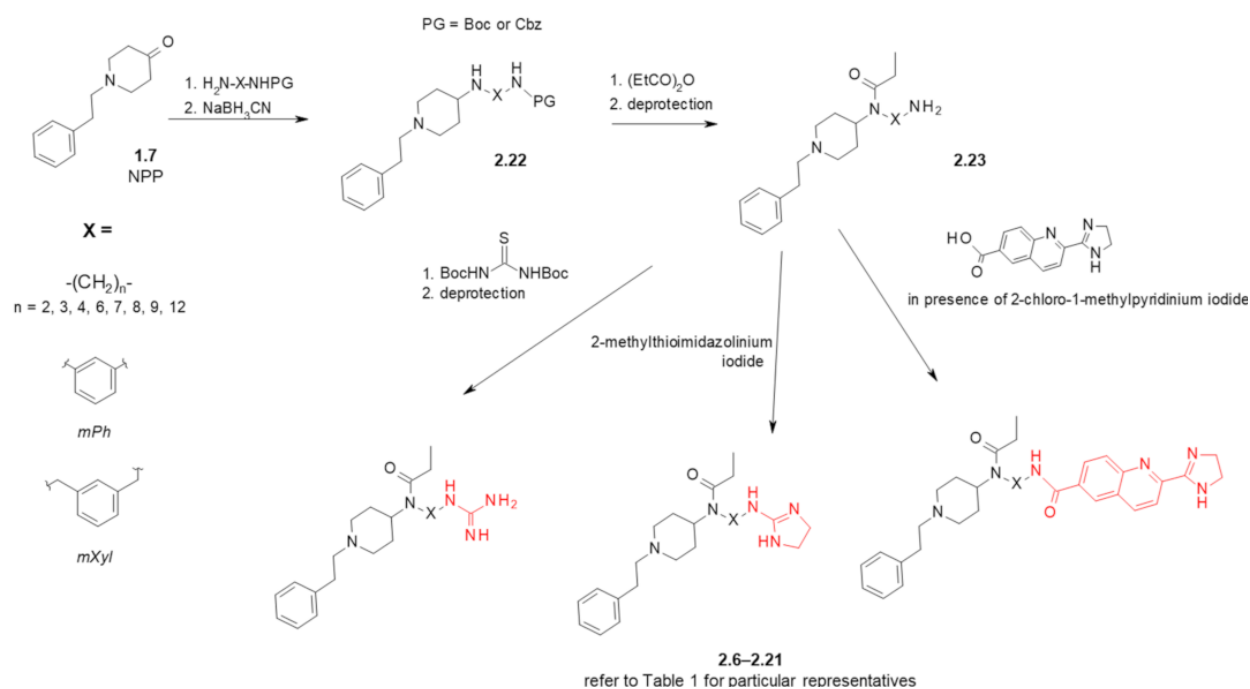


**Figure 3.** (A) Examples of typical I<sub>2</sub>-IBS ligands. In red marked are 2-aminoimidazoline, imidazoline and guanidine fragments characteristic for these compounds. (B) General scheme of fentanyl-based MOR/I<sub>2</sub>-IBS ligands based on the fentanyl scaffold. Refer to Table 1 for particular representatives.

Since some typical imidazoline receptor ligands (e.g., clonidine (2.2), agmatine (2.3), guanabenz (2.4), Figure 3A) contain guanidino or 2-aminoimidazolino groups in their structures, an attempt to achieve I<sub>2</sub> affinity was performed by introducing such groups into the fentanyl structure (Figure 3B and Table 1). First, these groups were either mounted on *meta*-position of the aromatic ring in region C (2.6 and 2.7) or connected to the amide nitrogen via spacer made of three -CH<sub>2</sub>- units (2.8 and 2.9) [26]. Following the initial activity data, the authors further explored SAR of the guanidine series by varying the length and the nature of the spacer (2.10–2.17) [27,28]. Finally, an I<sub>2</sub>-IBS selective ligand, BU224 (2.5) was coupled to the principal scaffold by aliphatic linkers of a variable length (2.18–2.21) [28].

The reported routes to the designed hybrids (Scheme 2 and Scheme S1 in Supplementary Materials) started with *N*-phenethyl-4-piperidinone (NPP, 1.7). NPP was subject to reductive amination with mono-protected diamines (or with 3-nitroaniline on the route to 2.6 and 2.7, Scheme S1). The resulting aminopiperidines (2.22) were acylated with propionic anhydride and deprotected with trifluoroacetic acid (for Boc-protected derivatives) or by catalytic hydrogenation (for Cbz-protected derivatives). The latter reaction served to reduce 3-nitro group to 3-amino group on the route to 2.6 and 2.7, too. Compounds 2.23 with a free amino group on an aliphatic or aromatic pendant were then (a) guanidinated with *N,N'*-di(*tert*-butyloxycarbonyl)thiourea and deprotected, (b) treated with 2-methylthioimidazolium iodide or (c) coupled with an acid derivative of BU224 in the presence of Mukaiyama's reagent (2-chloro-1-methylpyridinium iodide).



**Scheme 2.** Preparation of fentanyl-based MOR/ $\text{I}_2$ -IBS ligands. See Figure 3 and Table 1 for particular representatives. In red marked are fragments characteristic for  $\text{I}_2$ -IBS ligands. Boc—*tert*-butyloxycarbonyl, Cbz—carboxybenzyl.

**Table 1.** Affinities of fentanyl-based MOR/ $\text{I}_2$ -IBS ligands and reference compounds for the intended molecular targets.

Compound	Structure (Refer to Figure 3B for Structural Explanations)			Affinity [ $K_i$ (nM)] <sup>1</sup>		Ref.
	X	Y	$d_{\text{NC}}$ <sup>2</sup>	MOR <sup>3</sup>	$\text{I}_2$ -IBS <sup>4</sup>	
fentanyl (1.1)	-	-	-	$6 \pm 1.5$ <sup>5</sup>	$5462 \pm 1343$ <sup>6</sup>	[26]
				$2.9 \pm 1.5$	$8593 \pm 738$	[28]
idazoxan (2.1)	-	-	-	-	$307 \pm 183$ <sup>6</sup>	[26]
					$28 \pm 11$	[27,28]
BU224 (2.5)	-	-	-	-	$9.8 \pm 0.3$	[48]
2.6	mPh	gu	5	$7.8 \pm 2.5$ <sup>5</sup>	$1890 \pm 499$ <sup>6</sup>	[26]
2.7	mPh	amim	5	$7119 \pm 4089$ <sup>5</sup>	$9630 \pm 6731$ <sup>6</sup>	[26]
2.8	$-(\text{CH}_2)_3-$	gu	5	$37 \pm 12$ <sup>5</sup>	$2022 \pm 949$ <sup>6</sup>	[26]
				$23 \pm 4.5$	$1920 \pm 996$	[27]
2.9	$-(\text{CH}_2)_3-$	amim	5	$1751 \pm 1135$ <sup>5</sup>	$2327 \pm 811$ <sup>6</sup>	[26]
2.10	$-(\text{CH}_2)_2-$	gu	4	$433 \pm 83$	$437 \pm 228$	[27]
2.11	$-(\text{CH}_2)_4-$	gu	6	$0.59 \pm 0.18$	>10,000	[28]
2.12	$-(\text{CH}_2)_6-$	gu	8	$1.04 \pm 0.28$	$409 \pm 238$	[27]
2.13	$-(\text{CH}_2)_7-$	gu	9	$0.37 \pm 0.19$	$6627 \pm 3106$	[28]
2.14	$-(\text{CH}_2)_8-$	gu	10	$37 \pm 9.7$	$126 \pm 72$	[27]
2.15	$-(\text{CH}_2)_9-$	gu	11	$26 \pm 6$	$58 \pm 46$	[28]

Table 1. Cont.

Compound	Structure (Refer to Figure 3B for Structural Explanations)			Affinity [K <sub>i</sub> (nM)] <sup>1</sup>		Ref.
	X	Y	d <sub>NC</sub> <sup>2</sup>	MOR <sup>3</sup>	I <sub>2</sub> -IBS <sup>4</sup>	
2.16	-(CH <sub>2</sub> ) <sub>12</sub> -	gu	14	477 ± 75	6.5 ± 3.0	[27]
2.17	mXyl	gu	7	0.0098 ± 0.0033	>10,000	[28]
				0.448 ± 0.079 <sup>7</sup>		[49]
2.18	-(CH <sub>2</sub> ) <sub>3</sub> -	bu	12	6142 ± 2123	875 ± 713	[28]
2.19	-(CH <sub>2</sub> ) <sub>6</sub> -	bu	15	2168 ± 66	323 ± 270	[28]
2.20	-(CH <sub>2</sub> ) <sub>8</sub> -	bu	17	339 ± 35	>10,000	[28]
2.21	-(CH <sub>2</sub> ) <sub>12</sub> -	bu	21	545 ± 179	547 ± 316	[28]

<sup>1</sup> K<sub>i</sub>, inhibition constant (nM) with standard error of the mean, <sup>2</sup> d<sub>NC</sub>—topological distance (number of bonds) between the nitrogen attached at the position 4 of the piperidine ring and the central carbon atom in guanidine, 2-aminoimidazoline or imidazoline moieties, see Figure S1C, <sup>3</sup> unless specified otherwise, competitive assays done in membrane preparations of post-mortem human frontal cortex, 2 nM [<sup>3</sup>H]DAMGO as radioligand, <sup>4</sup> unless specified otherwise, competitive assays done in membrane preparations of post-mortem human frontal cortex, 1 nM [<sup>3</sup>H]2-BFI as radioligand, <sup>5</sup> competitive assays done in neural membrane preparations of mice brain, 2 nM [<sup>3</sup>H]DAMGO as radioligand, <sup>6</sup> competitive assays done in neural membrane preparations of mice brain, 1 nM [<sup>3</sup>H]2-BFI as radioligand, <sup>7</sup> competitive assays done in membrane preparations of rat brain, 0.72 nM [<sup>3</sup>H]DAMGO as radioligand.

The analogues with the guanidine moiety exhibited diversified MOR affinities with K<sub>i</sub>'s ranging from subnanomolar to single digit micromolar ones (Table 1). Guanidine derivatives with medium-length spacers (6–9 bonds) were of affinity similar or better than that of fentanyl (1.1). Shorter or longer spacers gave a monotonic decrease in binding affinity for guanidine-bearing analogues (Figure S1A in Supplementary Materials). Both considered 2-aminoimidazoline derivatives (2.7 and 2.9) had a MOR K<sub>i</sub> greater than 2 μM. In the cases of BU224 hybrids, the MOR K<sub>i</sub> varied between 339 and 6142 nM. The most potent MOR binder of the whole set was the guanidine derivative based on *meta*-xylene bridge (2.17) for which the authors reported a picomolar K<sub>i</sub> [28]. Later, this analogue (2.17) was retested by Weltrowska et al. [49] who found somewhat lower, but still subnanomolar MOR affinity (K<sub>i</sub> = 0.448 nM) [49]. Interestingly, compound 2.17 was found to possess an equally good binding to kappa opioid receptor (KOR, K<sub>i</sub> = 0.536 nM) [49].

According to our correlational analysis of the reported MOR affinities (Figure S1), there is a bilinear (or reversed U-shaped) dependence of the affinity on the linker length (particularly clearly seen for the guanidine series, Figure S1A). This suggests that in the MOR binding site there is a good interaction partner for guanidine/imidazoline that can be reached by the analogues in which these functions are attached at a linker of appropriate length. According to modelling by Weltrowska et al., such an interaction partner could be Asp216 side chain located at the second extracellular loop of MOR [49].

Regarding the affinity for I<sub>2</sub>-IBS, for fentanyl itself (1.1), K<sub>i</sub> values of 5462 and 8593 nM were found [26,28]. These values are significantly worse than the inhibition constants found for a reference I<sub>2</sub>-ligands like, idazoxan (2.1, K<sub>i</sub> = 307 nM [26] or K<sub>i</sub> = 28 nM [28]) or BU224 (2.5, K<sub>i</sub> = 9.8 nM [28]). Most of the fentanyl-hybrids had moderate to very low affinities. For only two of them (guanidine derivatives with nine or twelve methylene units in the linker, 2.15 and 2.16) the inhibition constants reported were below 100 nM. The analogues with 2-aminoimidazoline moiety (2.7 and 2.9) had low affinity (K<sub>i</sub> > 1 μM). All four BU224-based hybrids suffered a significant decrease in I<sub>2</sub>-IBS binding compared to their prototype, with K<sub>i</sub>'s from 323 nM to greater than 10,000 nM. Notably, a subnanomolar MOR binder 2.17 was reported to have K<sub>i</sub> > 10,000 nM at I<sub>2</sub>-IBS. If any SAR trend could be found in these data, this would be that for guanidine derivatives the I<sub>2</sub>-IBS affinity is positively correlated with the linker length (Figure S1B). Thus, the trend in I<sub>2</sub>-IBS affinity is not parallel to the putative trend for MOR affinities (Figure S1D) and optimizing the affinity ratios could not be expected with simple modulation of the linker lengths.

As to functional activity, analogues **2.6** and **2.8** assayed in isolated tissues (inhibition of electrically induced contractions in longitudinal muscle/myenteric plexus, LM/MP, from guinea pig ileum, GPI) turned out to be MOR agonists, however weaker than morphine (EC<sub>50</sub> values: 1.9 μM, 6.61 μM and 0.21 μM for **2.6**, **2.8** and morphine, respectively) [26]. Two compounds with high MOR affinity and tolerable I<sub>2</sub>-IBS affinity (**2.12** and **2.21**) were evaluated in [<sup>35</sup>S]GTPγS functional assays on membranes of post mortem human frontal cortex. The guanidine derivative **2.12** turned out to be a MOR agonist of rather low potency (25% stimulation of [<sup>35</sup>S]GTPγS binding; reverted by naloxone; EC<sub>50</sub> = 4.21 μM compared to DAMGO EC<sub>50</sub> = 77.1 μM). In the case of BU224-based analogue **2.21** much higher stimulation was observed (+ 125%), but the effect was not sensitive to the presence of naloxone, whence it can be concluded that this activity was MOR-independent.

The analogues **2.6**, **2.8** and **2.12** were tested further for analgesic activity in hot plate and writhing test in mice after the intraperitoneal administration (ip) [26,28]. The former two were relatively active in the writhing test (but less active than morphine), while inactive in the hot plate test (in nontoxic doses). Despite decent MOR affinity, compound **2.12** displayed no analgesic effect up to 40 mg/kg in either test and this high dosage turned out to be significantly lethal. The authors noted that this could be explained either based on rather low efficacy shown by **2.12** in the functional test or since a dicationic compound might have poor blood-brain barrier penetration.

### 3. Fentanyl-Based MTAs Targeting MOR and CB<sub>1</sub>R

The above-described research on MOR/I<sub>2</sub>-IBS ligands, apart from its important exploratory and pioneering character, produced SAR data and chemistry potentially useful for other attempts of ‘multitargeting’ with the fentanyl scaffold. The same Spanish group who generated these data used it to create molecules able to bind with MOR and cannabinoid 1 receptor (CB<sub>1</sub>R) [50].

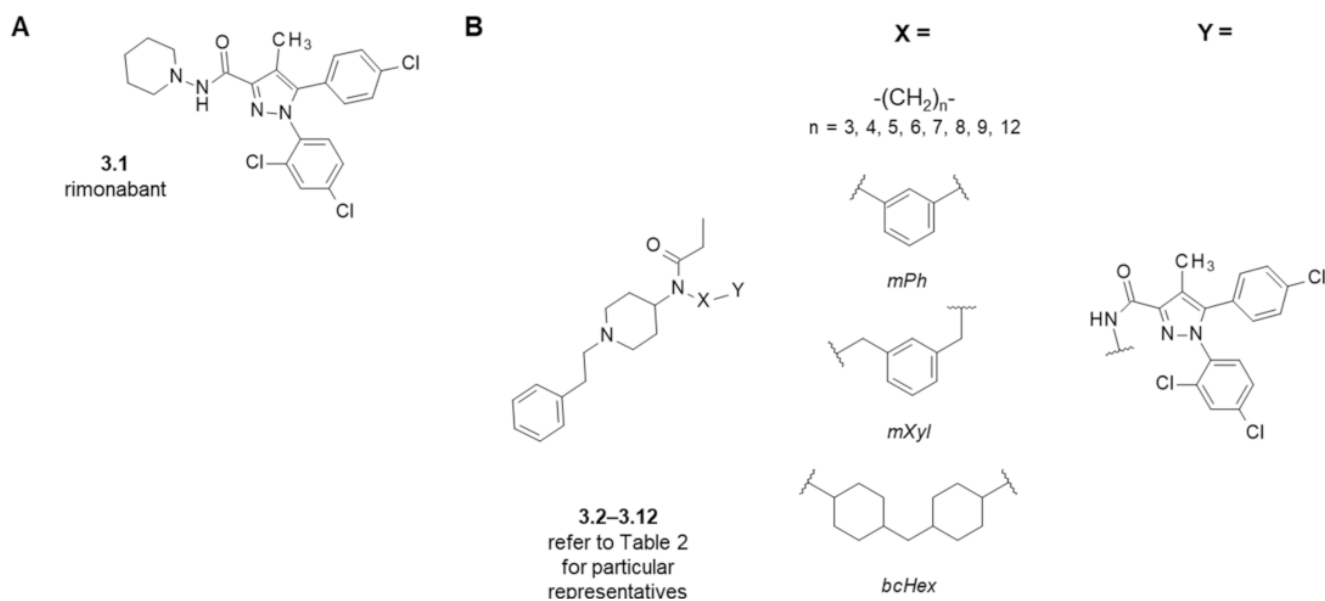
Just as MOR, CB<sub>1</sub>R is a GPCR widely expressed both in the CNS and in the periphery. Both receptors are involved in the control of nociception, mood, behaviour and food intake. There is much evidence on possible bidirectional interplay between cannabinoid receptors and MOR (nicely summarized in a review by Zádor and Wollemann [51]). The proteins are expressed in the same CNS areas, and they can be localized at the same neurons. In vitro, MOR/CB<sub>1</sub>R heterodimers are formed. Some CB<sub>1</sub>R antagonists reverse the morphine-induced analgesia, while antinociception produced with tetrahydrocannabinol (a CB<sub>1</sub>R/CB<sub>2</sub>R ligand) can be blocked with opioid antagonist naloxone. Importantly, development of tolerance to morphine may be inhibited by some CB<sub>1</sub>R antagonists [52]. These facts prompted the development of MOR/CBR hybrid ligands made of peptide or alkaloid opioid fragments linked to CB<sub>1</sub>R or CB<sub>1</sub>R/CB<sub>2</sub>R pharmacophores [10,11,53].

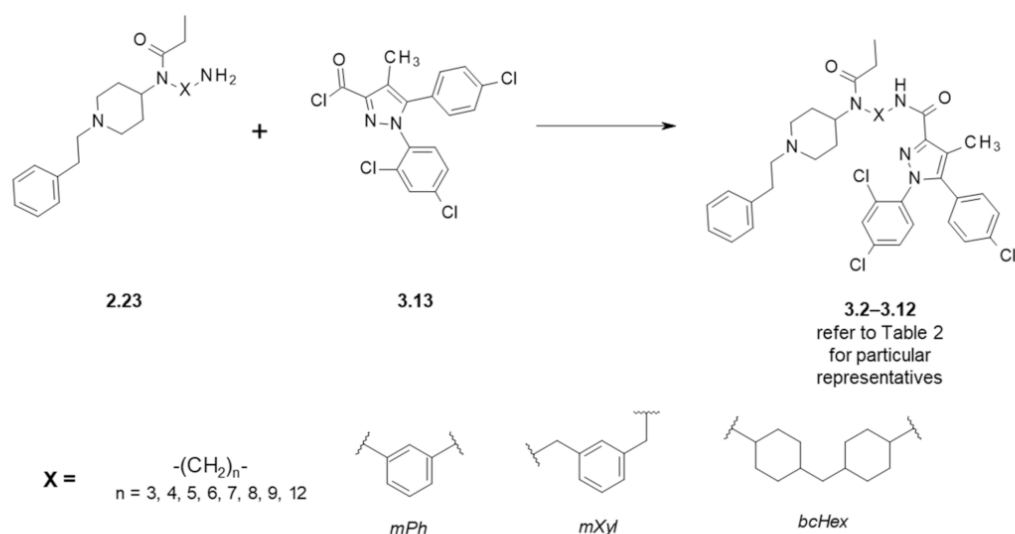
The attempt with the fentanyl scaffold [50] was meant to attach a CB<sub>1</sub>R pharmacophore by similar diamine linkers that previously had served to obtain compounds **2.6–2.21**. The CB<sub>1</sub>R fragment was based on rimonabant (**3.1**, Figure 4A), a selective CB<sub>1</sub>R inverse agonist/antagonist (once in clinical use but withdrawn). SAR studies of **3.1** suggested that replacement of the piperidine ring by alkyl chain was tolerated by CB<sub>1</sub>R. Hence, derivatives **3.2–3.12** were designed. Their synthesis (Scheme 3) utilized the intermediates (**2.23**) whose preparation was described earlier in the works on MOR/I<sub>2</sub>-IBS ligands (Scheme 2) [26–28]. To obtain **3.2–3.12** (Scheme 3), the free amino group of the appropriate analogues **2.23** was acylated by an acid chloride derivative of the rimonabant core (**3.13**).

**Table 2.** Affinities and antagonistic properties of fentanyl-based MOR/CB<sub>1</sub>R ligands and of reference compounds for the intended molecular targets. Data are from [50] unless specified otherwise.

Compound	Structure (Refer to Figure 4)	Affinity [K <sub>i</sub> (μM)] <sup>1</sup>		Antagonistic Properties (an Agonist's EC <sub>50</sub> in μM, [ <sup>35</sup> S]GTPγS Binding Assay <sup>2</sup> , in Presence of 10 μM of a Tested Compound)	
		MOR <sup>3</sup>	CB <sub>1</sub> R <sup>4</sup>	Fentanyl (Alone) EC <sub>50</sub> = 0.28 ± 0.04 μM	WIN55,212-2 (Alone) EC <sub>50</sub> = 1.1 ± 0.22 μM
Fentanyl (1.1)	-	0.003 ± 0.001	-	-	-
Rimonabant (3.1)	-	0.20 ± 0.12 <sup>5</sup>	0.004 ± 0.002	-	21 ± 3
Naloxone	-	-	-	456 ± 60	1.3 ± 0.17
3.2	-(CH <sub>2</sub> ) <sub>3</sub> -	3.81 ± 0.39	0.19 ± 0.07	-	-
3.3	-(CH <sub>2</sub> ) <sub>4</sub> -	1.23 ± 0.43	0.57 ± 0.20	24 ± 5	33 ± 8
3.4	-(CH <sub>2</sub> ) <sub>5</sub> -	0.17 ± 0.10	>10	-	-
3.5	-(CH <sub>2</sub> ) <sub>6</sub> -	0.30 ± 0.06	2.29 ± 1.86	33 ± 2	21 ± 2
3.6	-(CH <sub>2</sub> ) <sub>7</sub> -	6.54 ± 0.95	0.70 ± 0.57	3 ± 1	16 ± 2
3.7	-(CH <sub>2</sub> ) <sub>8</sub> -	1.24 ± 0.79	3.99 ± 1.37	-	-
3.8	-(CH <sub>2</sub> ) <sub>9</sub> -	0.11 ± 0.06	>10	-	-
3.9	-(CH <sub>2</sub> ) <sub>12</sub> -	6.90 ± 1.58	>10	-	-
3.10	mPh	1.25 ± 0.67	>10	-	-
3.11	mXyl	1.02 ± 0.25	>10	-	-
3.12	bcHex	0.66 ± 0.37	2.06 ± 0.60	-	-

<sup>1</sup> K<sub>i</sub>, inhibition constant (μM) with standard error of the mean, <sup>2</sup> [<sup>35</sup>S]GTPγS functional assays on cortical membranes of post mortem human brain, <sup>3</sup> competitive assays done in membrane preparations of post-mortem human prefrontal cortex, 2 nM [<sup>3</sup>H]DAMGO as radioligand, <sup>4</sup> competitive assays done in membrane preparations of post-mortem human prefrontal cortex, 1 nM [<sup>3</sup>H]CP55,940 as radioligand, <sup>5</sup> note also interesting contributions on the influence of rimonabant on opioid receptors in references: [54–56].

**Figure 4.** (A) Structure of a selective CB<sub>1</sub>R ligand, rimonabant. (B) General scheme of fentanyl-based MOR/CB<sub>1</sub>R ligands based on the fentanyl scaffold. Refer to Table 2 for particular representatives.



**Scheme 3.** Preparation of fentanyl-based MOR/CB<sub>1</sub>R ligands. See Table 2 for particular representatives.

Binding affinity assays (Table 2) revealed that all hybrids 3.2–3.12 had diminished CB<sub>1</sub>R affinity compared to rimonabant (3.1). Submicromolar K<sub>i</sub>'s at cannabinoid 1 receptor were found for propyl (3.2), butyl (3.3) and heptyl-based (3.6) compounds, whereas the longest derivatives (3.8 and 3.9) or those with aromatic spacers (3.10 and 3.11) did not appreciably bind to the receptor. For the alkyl derivatives, an approximate, linear, negative relationship between the linker chain length and CB<sub>1</sub>R affinity can be proposed (Figure S2B).

As to the MOR affinity, the hybrids were significantly worse binders than the parent fentanyl (1.1) or the corresponding guanidine derivatives (2.6–2.16) from MOR/I<sub>2</sub>-IBS works [26–28]. The K<sub>i</sub> ranged from ~100 nM to ~7 μM. Submicromolar values were found for 3.4, 3.5, 3.8 and 3.12. If the pK<sub>i</sub>'s are plotted against the chain length, a zig-zag pattern with two optima could be supposed (Figure S2A). This would suggest the existence of two separate subsites in which rimonabant fragment could enjoy relatively favourable interactions with the MOR (Figure S2C). Again, as in the MOR/I<sub>2</sub>-IBS hybrids, the affinity trends for CB<sub>1</sub>R and MOR are not parallel (Figure S2D).

The compounds 3.3, 3.5 and 3.6 were advanced to functional assays ([<sup>35</sup>S]GTPγS binding). Consistently with the design assumption, they were found to be CB<sub>1</sub>R antagonists of potency similar to that of rimonabant [50]. Quite surprisingly however, these analogues turned out to be opioid antagonists. For 3.5 and 3.6, tentative behavioural *in vivo* tests confirmed the CB<sub>1</sub>R and MOR antagonistic properties. In mice, the compounds 3.5 (4 mg/kg ip) and 3.6 (5 mg/kg ip) were able to antagonise the effects that WIN55,212-2 (a potent cannabinoid agonist; at dose 1.5 mg/kg) had on rectal temperature, catalepsy, pain perception and spontaneous activity. Similarly, they blocked morphine analgesia in a hot plate test (10 mg/kg ip prior to 10 mg/kg morphine, ip). Since both CB<sub>1</sub>R and MOR antagonism is known to influence alcohol dependence [57], the authors checked if 3.6 could affect ethanol self-administration (alcohol relapse model in Wistar rats), but no significant effect was observed up to 8.0 mg/kg.

The MOR antagonism confirmed for a few analogues seems particularly worth noting since opioid antagonism in fentanyl-based compounds is rather uncommon. In the numerous family of fentanyls, only few such examples are known [58,59]. This is in marked contrast to the alkaloid opioid receptor ligands, among which many compounds with varying functional properties have been described.

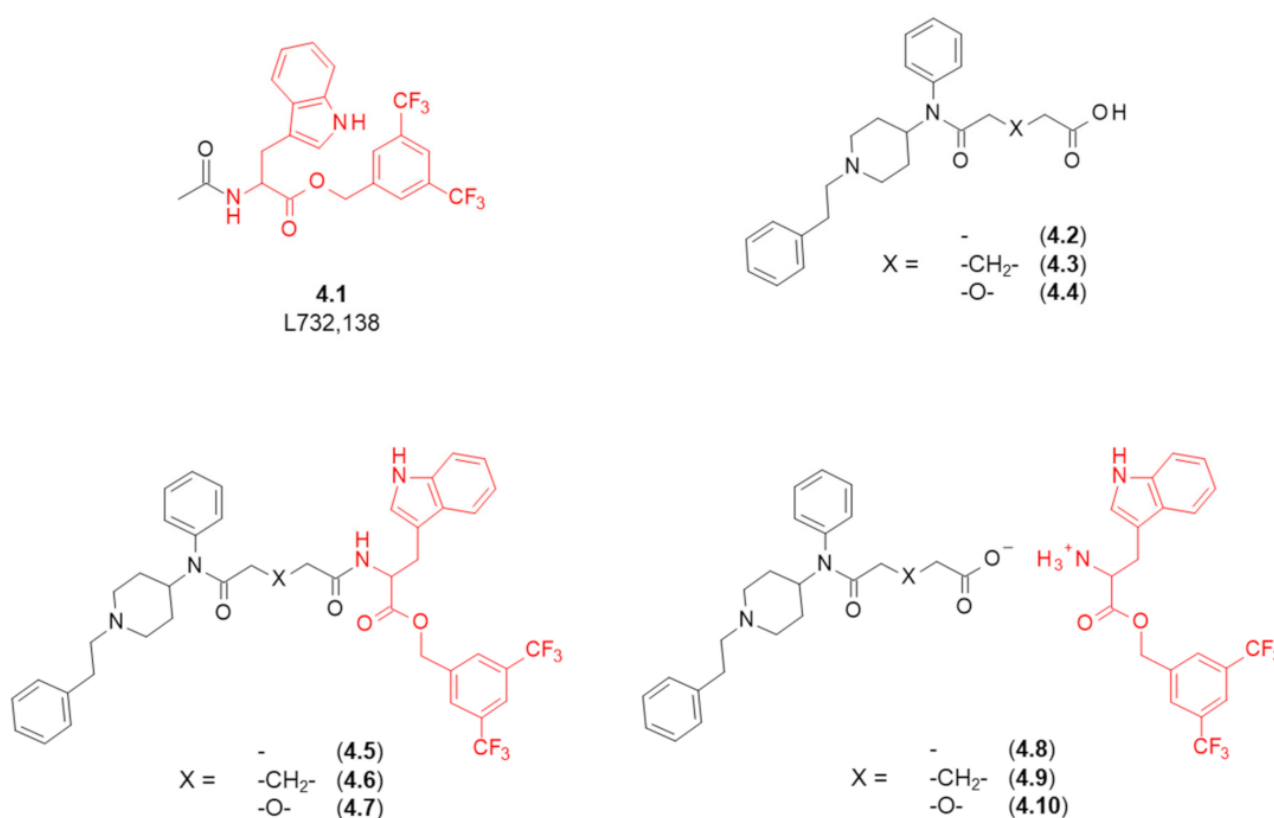
#### 4. Fentanyl-Based MTAs Targeting MOR and NK<sub>1</sub>R

A GPCR which has been many times used as a second target for MTAs is the NK<sub>1</sub> tachykinin receptor (NK<sub>1</sub>R). An endogenous agonist of this receptor, Substance P (SP), is a sensory neurotransmitter involved in the pain perception, usually considered to be a

pronociceptive factor [60]. Upregulation of SP and NK<sub>1</sub>R after prolonged opioid intake as well as in the chronic pain conditions is believed to be involved in the development of central sensitization, hyperalgesia and opioid analgesic tolerance [61,62]. Simultaneous administration of NK<sub>1</sub>R antagonists with opioid agonists was reported to give improved antinociceptive response and to prevent antinociceptive tolerance [63]. On the other hand, there are some data which indicate that in certain conditions SP, its metabolites or selective NK<sub>1</sub>R agonists could have analgesic activity, too [64].

Hence, many opioid/NK<sub>1</sub>R multifunctional ligands were prepared and tested. These contained both peptide and organic structural fragments and were intended to exhibit either agonistic or antagonistic properties at the NK<sub>1</sub>R. A review of the NK<sub>1</sub>R-related multifunctional analgesics and a critical evaluation of the concept was provided recently by Kleczkowska et al. [12].

Vardanyan et al. examined whether dual MOR/NK<sub>1</sub>R ligands could be created using the fentanyl scaffold [65]. The NK<sub>1</sub>R pharmacophoric fragment to be employed was based on the structure of one of the early potent NK<sub>1</sub>R antagonists, L732,138 (4.1, Figure 5, [66]). The authors chose carboxyfentanyl (4.2) and its two analogues (4.3–4.4) to serve for attaching the NK<sub>1</sub>R-related fragment by an amide bond in the D region (4.5–4.7). A rather infrequent idea to develop ionic pairs (4.8–4.10) was pursued, too. In these, the fentanyl-related carboxylates were paired with aminium derivative (4.11, Scheme 4) related to 4.1.

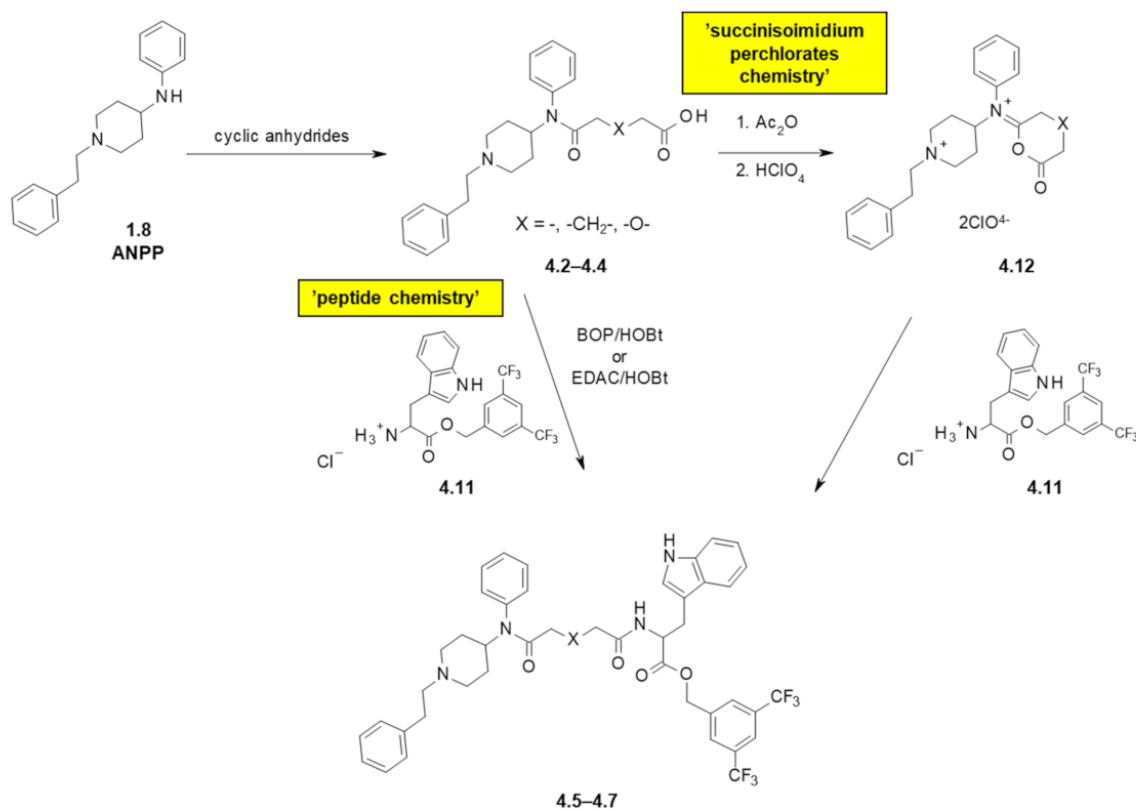


**Figure 5.** Structures of NK<sub>1</sub>R antagonist L732,138, carboxylate derivatives of fentanyl and of the designed fentanyl-based MOR/NK<sub>1</sub>R ligands. In red marked are fragments responsible for NK<sub>1</sub>R binding.

**Table 3.** Receptor affinities and functional data for fentanyl-based opioid/NK<sub>1</sub>R MTAs. Data from [65].

Structure	X (Refer to Figure 5)	Affinity [K <sub>i</sub> (nM)] <sup>1</sup>		Functional Tests (Inhibition of the Contractile Response Generated by Electrical Stimulation)		
		MOR <sup>2</sup>	NK <sub>1</sub> R <sup>3</sup>	MOR (GPI/LM/MP) <sup>4</sup>	DOR (MVD) <sup>5</sup>	NK <sub>1</sub> R (GPI/LM/MP) <sup>4</sup>
				Opioid Agonism, Inhibition of Contraction Height (% at 1 μM or IC <sub>50</sub> in nM)		Antagonism of SP Action <sup>6</sup> [K <sub>e</sub> ± SEM (nM)] (at 1 μM)
<b>Covalently linked compounds</b>						
4.5	-	130	13	410 ± 42 nM	14%	240 ± 39
4.6	-CH <sub>2</sub> -	120	6.8	55 ± 12 nM	13%	21 ± 4.3 (at 100 nM)
4.7	-O-	400	31	30%	30%	480 ± 12
<b>Ionic pairs</b>						
4.8	-	>10,000	21	1.8%	4.3%	210 ± 42
4.9	-CH <sub>2</sub> -	3900	44	19.5%	19.8%	500 ± 130
4.10	-O-	1300	23	11%	17.1%	490 ± 68

<sup>1</sup> K<sub>i</sub>, inhibition constant, <sup>2</sup> competitive assays using [<sup>3</sup>H]DAMGO as radioligand, done in membrane preparations from cells expressing human MOR, <sup>3</sup> competitive assays using 0.5 nM [<sup>3</sup>H]-Substance P as radioligand, done in membrane preparations of CHO cells stably transfected with human NK<sub>1</sub>R, <sup>4</sup> longitudinal muscle/myenteric plexus (LM/MP) of the guinea pig ileum (GPI), <sup>5</sup> isolated mouse vas deferens (MVD), <sup>6</sup> longitudinal muscle/myenteric plexus assay in presence of Substance P.

**Scheme 4.** Preparation of fentanyl-based MOR/NK<sub>1</sub>R ligands. See Figure 5 and Table 3 for particular representatives. BOP—benzotriazole-1-yl-oxytris(dimethylamino)-phosphonium hexafluorophosphate, HOBt—1-hydroxybenzotriazole, EDAC—1-ethyl-3-(3-dimethylaminopropyl)carbodiimide.

The carboxylates (4.2–4.4) were synthesized (Scheme 4) by acylating 1.8 with appropriate cyclic anhydrides. The desired covalent hybrids (amides 4.5–4.7) were then obtained by coupling the amine 4.11 following a typical peptide chemistry approach (carboxyl activation by a carbodiimide or a phosphonium salt). An interesting alternative based on succinisoimidium perchlorates chemistry was developed, too. In this route, the acids (4.2–4.4) were treated with acetic anhydride and perchloric acid to give isoimidium perchlorates (4.12). These were then reacted with a hydrochloride aminium 4.11 to yield the desired hybrids. Finally, the ionic pairs (4.8–4.10) were obtained by simple mixing the potassium salts of 4.2–4.4 and the hydrochloride aminium 4.11.

The obtained covalent hybrids turned out to have moderate MOR affinity (Table 3), with  $K_i$ 's being 400 nM in the case of an ether derivative (4.7) or slightly greater than 100 nM in the cases of 4.5 and 4.6. On the other hand, the ionic compounds exhibited MOR  $K_i$ 's greater than 1  $\mu$ M, what suggests that an acidic moiety in the region D of fentanyl is highly unfavourable to MOR binding. As to the NK<sub>1</sub>R binding, both the covalent and the ionic compounds had low nanomolar affinity, with  $K_i$ 's ranging 6.8–44 nM. The compound 4.6 had the lowest  $K_i$  values in binding to both receptors.

Consistently with the affinity data, the hybrids had weak or very weak agonistic (and no antagonistic) activity at opioid receptors in isolated tissues. In the NK<sub>1</sub>R functional assays, they were found to antagonise the effects of SP, with 4.6 being the most efficient in this. As this analogue exhibited some moderate MOR affinity and agonism too, the authors concluded that 4.6 could serve as a lead compound. They pointed that elongation and other variations in the connecting spacer (e.g., insertion of a peptide fragment) will be a direction for further work.

## 5. Fentanyl-Based MTAs Targeting MOR and D<sub>2</sub>-like Dopamine Receptors

Other non-opioid GPCRs which are of interest as potential co-targets for multifunctional analgesics are D<sub>2</sub>-like dopamine receptors (D<sub>2</sub>-likeRs). This subfamily includes D<sub>2</sub>, D<sub>3</sub> and D<sub>4</sub> dopamine receptors. These proteins and MOR exhibit co-distribution in several parts of the brain [67]. There is in vitro evidence that suggests the existence of D<sub>2</sub>R-MOR and D<sub>4</sub>R-MOR heterodimers [68]. Moreover, there are reports on the cross-regulation of opioid and dopaminergic system, in particular in reward processes [69–74].

In the light of these facts, simultaneous targeting of MOR and D<sub>2</sub>-likeRs (as separate receptors or as heterodimers) may be a basis for innovative, nonaddictive analgesics. Qian et al. demonstrated feasibility of targeting MOR/D<sub>2</sub>-likeRs heterodimers by long molecules containing alkaloid MOR-related fragments (naltrexone, hydromorphone) [68]. Bonifazi et al. synthesized MOR-D<sub>3</sub>R bitopic/bivalent compounds in which opioid fragment was based on acyclic opioids [75].

The possibility to employ a substructure of fentanyl (4-anilidopiperidine) in MOR/D<sub>2</sub>R multitarget ligands was investigated by Jevtić et al. [76,77]. The D<sub>2</sub>R pharmacophoric element to be incorporated was *N*-arylpiperazine which is present in D<sub>2</sub>R ligands such as aripiprazole (5.1, Figure 6) or pibedil (5.2). This element was installed (5.3–5.18) in region B of fentanyl structure by alkyl chains of variable length (2 up to 6 methylene units).

The synthetic approach devised at first was intended to consist of two alkylations of secondary amines in piperazine and piperidine derivatives. In this approach, norfentanyl (5.19, Scheme S2) reacted with  $\alpha,\omega$ -bromochloroalkanes, but instead of desired linear products it was spiro-bicyclic quaternary ammonium salts that were formed (Scheme S2). In the alternative approach (Scheme 5), *N*-arylpiperazines (5.20) were subject to acylations with  $\omega$ -bromoacyl chlorides, and the resulting bromides (5.21) served for *N*-alkylation of 4-anilino-piperidine (5.22). In the latter step, quite large amounts of *N,N'*-dialkylated products were also observed with the second alkylation taking place at the anilino nitrogen. After removing these impurities, borane reduction of the tertiary carboxamido group in 5.23 gave compounds 5.24 that were acylated with propionyl chloride to yield the designed compounds (5.3–5.18).

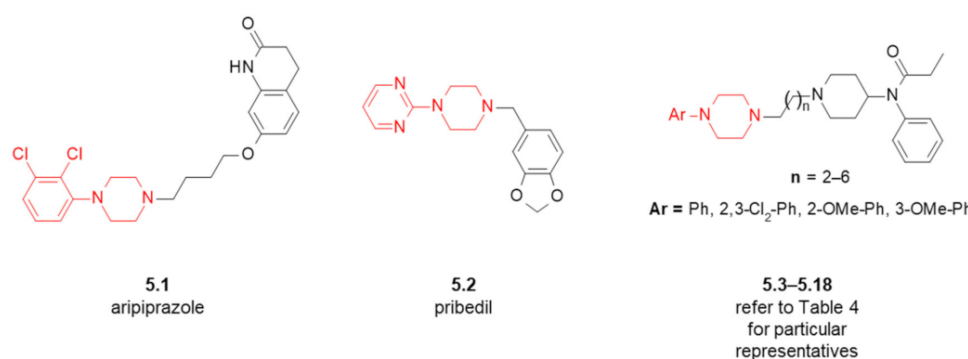


**Figure 6.** Structures of dopamine receptor ligands and of the designed fentanyl-based MOR/D<sub>2</sub>R MTAs. In red marked are fragments characteristic for D<sub>2</sub>R-ligands.

**Table 4.** Affinity fentanyl-based MOR/D<sub>2</sub>R MTAs. Data taken from [77].

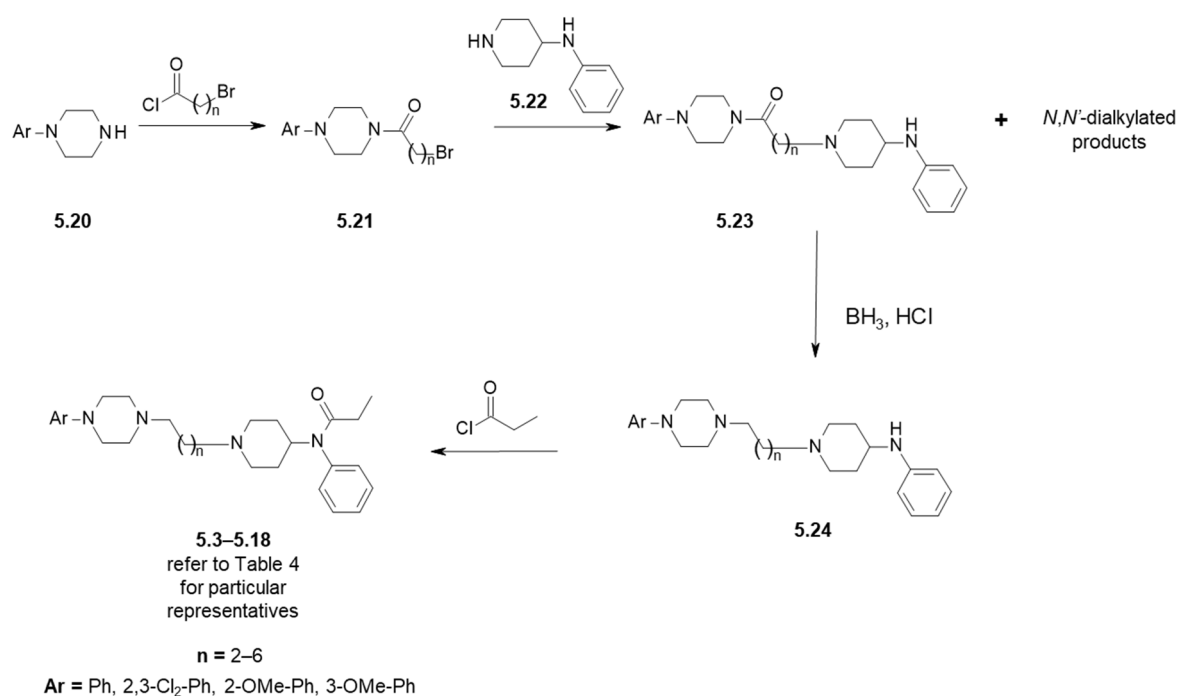
Compound	Ar (Refer to Figure 6)	n	D <sub>2</sub> R Receptor Binding, [K <sub>i</sub> (nM)] <sup>1</sup>
5.3	Ph	2	869
5.4	2-OMe-Ph	2	800
5.5	2,3-Cl <sub>2</sub> -Ph	2	594
5.6	Ph	3	1357
5.7	2-OMe-Ph	3	7992
5.8	3-OMe-Ph	3	n/d <sup>2</sup>
5.9	2,3-Cl <sub>2</sub> -Ph	3	6956
5.10	Ph	4	7083
5.11	2-OMe-Ph	4	4436
5.12	2,3-Cl <sub>2</sub> -Ph	4	2376
5.13	Ph	5	8105
5.14	2-OMe-Ph	5	3778
5.15	2,3-Cl <sub>2</sub> -Ph	5	1500
5.16	Ph	6	1853
5.17	2-OMe-Ph	6	5454
5.18	2,3-Cl <sub>2</sub> -Ph	6	5326

<sup>1</sup> K<sub>i</sub>, inhibition constant, competitive radioligand binding assay with 0.2 nM [<sup>3</sup>H]-spiperone as radioligand, in preparations of rat caudate nuclei synaptosomal membranes, <sup>2</sup> n/d—not determined.

The prepared analogues were tested *in vitro* for binding to dopamine receptors and *in vivo* for their antinociceptive activity (in rats, using tail-immersion test after ip injection). In the latter of the performed test, antinociceptive activity in doses up to 2 mg/kg was absent. Not necessarily does this exclude MOR affinity of the studied compounds, since as the authors noted themselves, physicochemical properties of the compounds or their metabolism could impair distribution into CNS. Hence, further research programmes based on these analogues require that MOR affinity is measured.

With regard to dopamine receptor binding, the studied analogues showed rather moderate affinity with K<sub>i</sub> ranging from 594 nM to 8105 nM (Table 4). The best (submicromolar) affinities were observed for the shortest compounds (with three methylene units as a linker, n = 2, 5.3–5.5). Elongation of the linker resulted in deterioration of binding strength (Figure S3A) so that none of the compounds with n > 2 exhibited submicromolar K<sub>i</sub>. The effect of substituents on the N-aryl ring seems non-additive to the effect of chain elongation (see Figure S3B–D and below for our QSAR analysis). When n = 2, 4 or 5, the

following binding preference is found  $2,3\text{-Cl}_2\text{-Ph} > 2\text{-OMe-Ph} > \text{Ph}$ . On the other hand, for  $n = 3$  or  $6$ , analogues with unsubstituted phenyl have much better affinity than those with the substitutions present, and so the preference is  $\text{Ph} \gg 2,3\text{-Cl}_2\text{-Ph} \sim 2\text{-OMe-Ph}$ . This could suggest a binding mode switch with the length of the linker. Jevtić conducted preliminary docking analysis of a few analogues with the intent of explaining the observed  $\text{D}_2\text{R}$  affinities [78]. An important observation is that while the arylpiperazine moiety resides deep in the orthosteric pocket, while the anilidopiperidine moiety is located in the extended binding pocket. The key polar interaction with Asp114 (expected for high affinity at  $\text{D}_2\text{R}$ ) is formed, but it may be of suboptimal geometry and for this reason, the  $\text{D}_2\text{R}$  affinity is rather moderate. The obtained binding models might serve for further optimization of the affinities.



**Scheme 5.** Preparation of fentanyl-based MOR/ $\text{D}_2\text{R}$  ligands. See Table 4 for particular representatives.

As a side note, let us mention that an avenue that might deserve exploration is using fentanyl scaffold for designing compact ('merged') MOR/ $\text{D}_4\text{R}$  multifunctional drugs. Fentanyl (**1.1**) has been recently shown to have almost no  $\text{D}_2\text{R}$  ( $K_i = 21,000$  nM) and no  $\text{D}_3\text{R}$  binding ( $K_i = 26,200$  nM), but some moderate, submicromolar affinity for  $\text{D}_4\text{R}$  ( $K_i = 554$  nM) [75].

## 6. Fentanyl-Based MTAs Targeting MOR and COX

Not only receptors but also enzymes are considered as targets for the MTAs, however these attempts (at least in combination with opioid receptors as co-targets) seem less frequent. There is a single report by Vardanyan et al. [23] on ligands designed to be MOR agonists and inhibitors of cyclooxygenases (COXs). COXs are enzymes involved in the production prostaglandins from arachidonic acid, and in this way, they participate in the inflammatory and pain reactions. Inhibition of COXs is the main mechanism of action for the non-steroidal anti-inflammatory drugs (NSAIDs) which are popular analgesic compounds with anti-inflammatory and antipyretic action. NSAIDs and opioids are sometimes used together in multimodal management of pain because of the purported synergistic effect [79], and in some markets available are fixed-dose opioid/NSAIDs combinations. Multitarget opioid receptors/COX-targeting analgesics could be in principle superior to these for the reasons of dosing convenience and pharmacokinetics.

Vardanyan et al. [23] attempted creating such hybrids by combining fragments of fentanyl with the indolyl/indene acetic acid motif present in some NSAIDs, such as indomethacin (6.1, Figure 7A) sulindac (6.2) or L748,780 (6.3). The motif was to be melted into C and D region of fentanyl structure to give compounds (6.4–6.9).

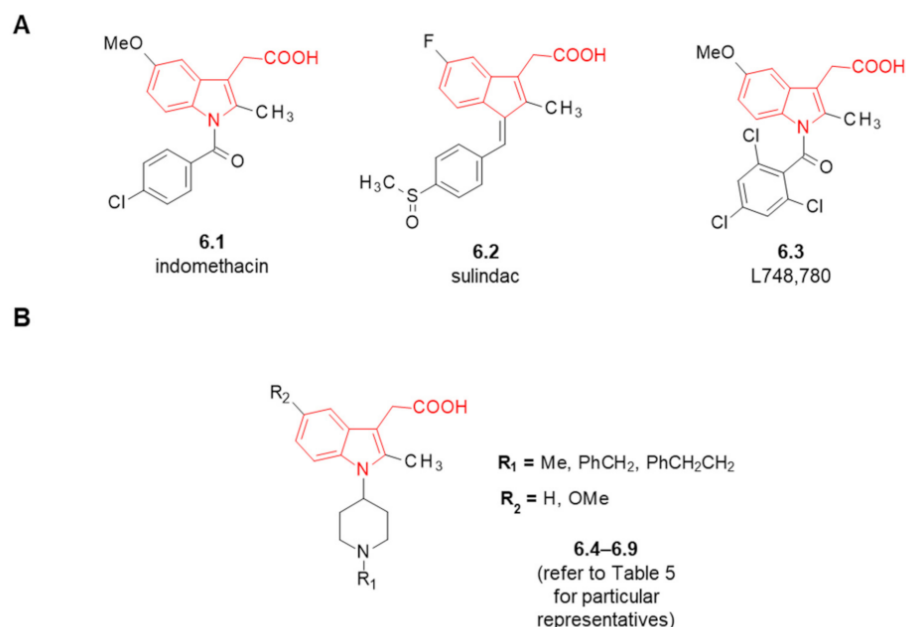


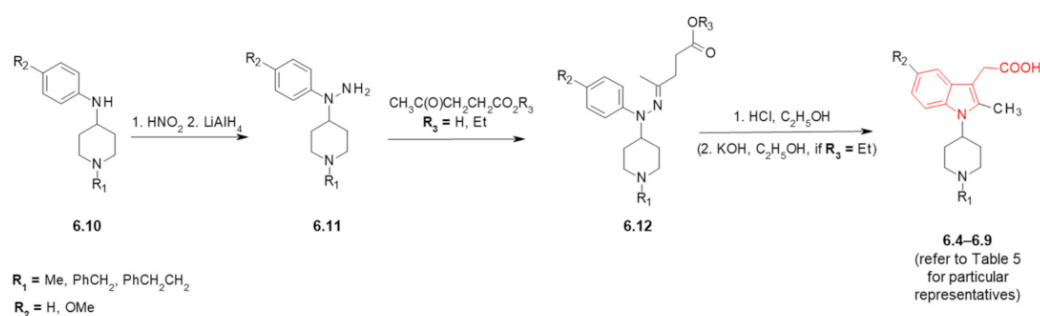
**Figure 7.** (A) Structures of COX inhibitors. (B) Structures of the designed fentanyl-based MOR/COX MTAs. In red marked is indolyl/indene acetic acid motif.

On the route to these analogues (Scheme 6), appropriate *N*-substituted 4-anilinpiperidines (6.10) were subject to nitrosylation with HNO<sub>2</sub> and the resulting *N*'-nitroso derivatives were hydrogenated to obtain hydrazines (6.11). By condensation of these with levulinic acid or its esters, hydrazones (6.12) were formed which in the presence of HCl in ethanol converted to indole derivatives with the desired substitution pattern (6.4–6.9).

**Table 5.** Opioid activities of fentanyl-based MOR/COX MTAs. Data from [23].

Compound	Structure (Refer to Figure 7)	Functional Tests (Inhibition of the Contractile Response Generated by Electrical Stimulation)	
		DOR (MVD <sup>1</sup> )	MOR (GPI/LM/MP <sup>2</sup> )
	R <sub>1</sub>	R <sub>2</sub>	Opioid Agonism, Inhibition of Contraction Height (% at 1 μM or IC <sub>50</sub> in nM)
6.4	Me	H	17.9%      0.7%
6.5	PhCH <sub>2</sub>	H	IC <sub>50</sub> = 1266 ± 355 nM      IC <sub>50</sub> = 5164 ± 2043 nM
6.6	PhCH <sub>2</sub> CH <sub>2</sub>	H	19.5%      3.1%
6.7	Me	OMe	2.8%      0%
6.8	PhCH <sub>2</sub>	OMe	8.3%      3%
6.9	PhCH <sub>2</sub> CH <sub>2</sub>	OMe	0%      6%

<sup>1</sup> isolated mouse vas deferens (MVD), <sup>2</sup> longitudinal muscle/myenteric plexus (LM/MP) of the guinea pig ileum (GPI).



**Scheme 6.** Preparation of fentanyl-based MOR/COX ligands. See Table 5 for particular representatives. In red marked is indolyl motif characteristic for COX inhibitors.

Unfortunately, the expected dual activity was not confirmed in the biological assays (Table 5). The analogues exhibited very low opioid activity, as measured by assays in tissue preparations (GPI/LM/MP and MVD). For only one of them (6.5,  $R_1 = \text{PhCH}_2$ ,  $R_2 = \text{H}$ ) micromolar  $\text{IC}_{50}$ s were established (GPI/LM/MP  $\sim 5 \mu\text{M}$ , MVD  $\sim 1 \mu\text{M}$ ). None of the compounds had antagonistic activity at MOR and DOR at  $1 \mu\text{M}$ .

Regarding the COX inhibition, the compounds tested at a concentration of  $50 \text{ nM}$  did not inhibit production of prostaglandin by COX-1 or COX-2. In line with the receptor/enzyme data, the compounds showed no in vivo antinociceptive activity in rat models of acute and chronic pain ( $10 \mu\text{g}$ , intrathecal).

The authors related the lack of opioid activity to conformational differences in fentanyl and the indole-incorporating derivatives (on comparing the crystal structures of fentanyl 1.1 and of an ester derivative of 6.6).

## 7. Fentanyl-Based MTAs Targeting MOR and FAAH/MAGL Hydrolases

Other enzymes that are relevant to the subject of this review are fatty acid amide hydrolase (FAAH) and monoacylglycerol lipase (MAGL). FAAH and MAGL are hydrolases that participate in the catabolism of endocannabinoids. Their inhibition increases levels of endogenous cannabinoids and in this way it may bring antinociception [80]. Indeed, blocking of FAAH or MAGL was demonstrated to result in analgesic activity in different pain models [81,82]. Several FAAH and MAGL inhibitors were advanced to clinical trials (in indications related to pain, but not only thereto), but as of today it did not result in approved drugs [83]. Both enzymes attract attention in the multitarget approach, too.

Monti et al. proposed two series of fentanyl-related analogues 7.1–7.12 in which *N*-arylurea or *O*-arylcarbamate substructures were melted in region D of the fentanyl structure (Figure 8A) [24]. Both these motifs are present in either FAAH or MAGL inhibitors [84] (e.g., 7.13–7.15, Figure 8B). The synthesis of fentanyl-derivatives 7.1–7.12 (Scheme 7) was accomplished by reacting 4-anilino-*N*-phenethylpiperidine (ANPP, 1.8) with appropriate chloroformates (7.16) or *N*-arylcarbamoyl chlorides (7.17).

The MOR affinities of the synthesized compounds were at best moderate (Table 6). In no case was  $\text{IC}_{50}$  better than  $500 \text{ nM}$ . The best binding derivative, undecorated urea 7.7, had  $\text{IC}_{50} = 516 \text{ nM}$ . Slightly worse values were found for 7.3, ( $X = \text{O}$ ,  $Y = 3\text{-Cl}$ ) 7.8, 7.9 ( $X = \text{NH}$ ,  $Y = 4\text{-Cl}$  or  $3\text{-Cl}$ ). A dramatic deterioration in MOR affinity was found upon introduction of 4-*t*Bu substituent in the urea series (7.10) leading to  $\text{IC}_{50} > 20,000 \text{ nM}$ . No general SAR trend regarding MOR affinity can be found in this series, except perhaps for stating that the effect of the substituent is not additive to the effect of urea/carbamate linker (Figure S4). According to the modelling performed by Monti et al. [24], the analogues 7.1–7.12 bind to MOR in a manner only partially matching the binding mode of fentanyl which could explain moderate affinity and different functional properties.

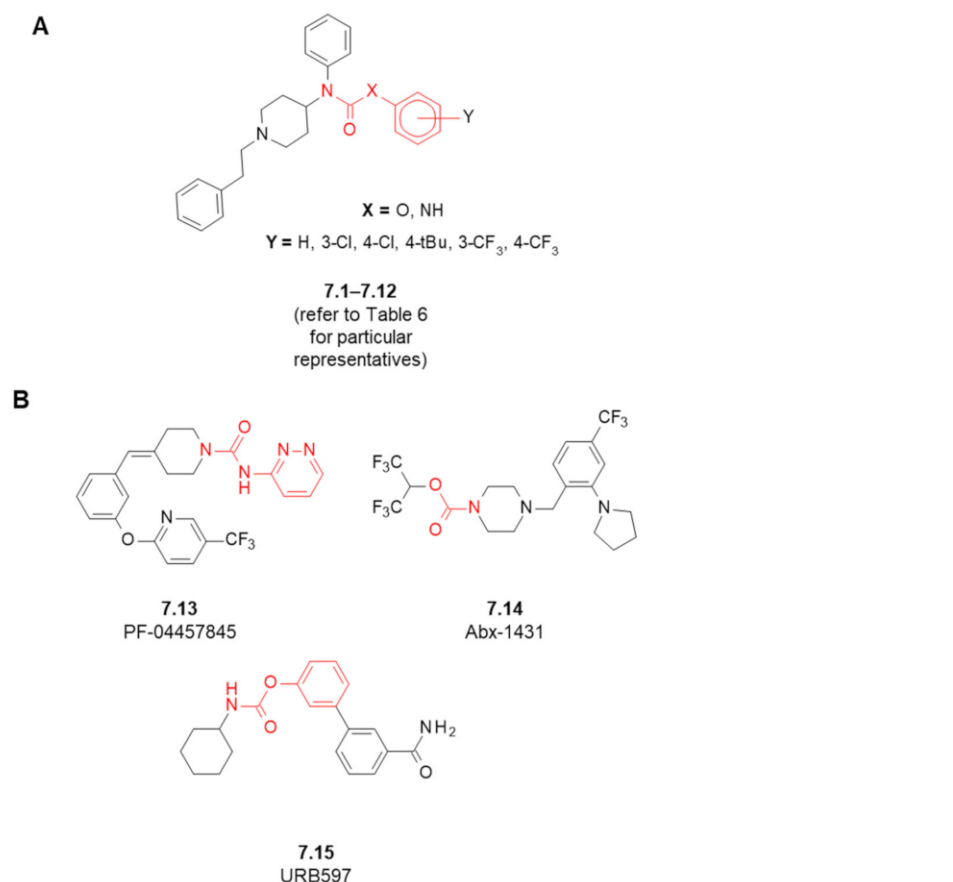
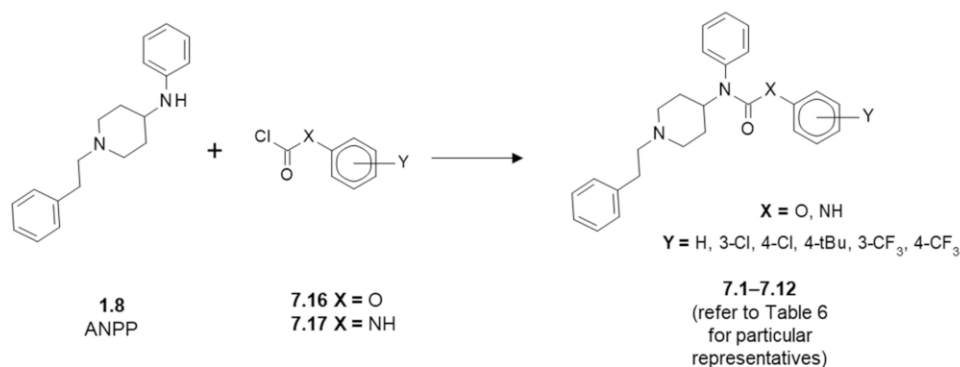


**Figure 8.** (A) Structures of the designed fentanyl-based MOR/FAAH/MAGL MTAs. (B) Structures of selected FAAH/MAGL inhibitors. In red marked is carbamate/urea substructures.



**Scheme 7.** Synthesis of fentanyl-based MOR/FAAH/MAGL ligands.

Regarding the enzymatic activity (Table 6), the analogues did not affect the activity of either FAAH or MAGL. Only trace signs of inhibition were found at concentration as high as 10  $\mu$ M. Moreover, the authors examined if compounds 7.2 and 7.3 could bind to DOR, KOR and CB<sub>1</sub>R, in all cases finding IC<sub>50</sub> values in the micromolar ranges.

In the functional assay ([<sup>35</sup>S]GTP $\gamma$ S binding), all the novel analogues turned out to be inverse agonists properties, reducing G-protein basal activity (efficacy in the range 80–100%, potency in the range 3–5  $\mu$ M). The effect was not reversed by the opioid antagonist naloxone. All in all, this suggests that the studied derivatives are active against some other, non-opioid molecular target of the GPCR family. Interestingly, two compounds (7.2 and 7.3) were found to have some antinociceptive activity in vivo in hot plate test in mice, but only at high doses, and with no apparent relationship to opioid receptor affinity or to enzymatic inhibition.

**Table 6.** Biological data for the designed fentanyl-based MOR/FAAH/MAGL ligands for the intended molecular targets. Data are from [24].

Compound	Structure (Refer to Figure 8)		MOR Affinity [IC <sub>50</sub> (nM)] <sup>1</sup>	Maximal Inhibition at 10 μM [%]	
	X	Y		FAAH <sup>2</sup>	MAGL <sup>3</sup>
fentanyl (1.1)	-	-	5.99	n/d <sup>4</sup>	n/d
7.1	O	-	1442	0	0
7.2	O	4-Cl	2180	0	0
7.3	O	3-Cl	654.2	1.90	0
7.4	O	4-tBu	1830	10.2	0.74
7.5	O	4-CF <sub>3</sub>	2657	7.40	0
7.6	O	3-CF <sub>3</sub>	4093	7.40	0.41
7.7	NH	-	516.8	7.25	0
7.8	NH	4-Cl	665.1	8.26	3.50
7.9	NH	3-Cl	658.9	9.76	7.32
7.10	NH	4-tBu	23,050	5.82	1.28
7.11	NH	4-CF <sub>3</sub>	4031	7.49	0
7.12	NH	3-CF <sub>3</sub>	1204	9.16	2.97

<sup>1</sup> competitive assays done in rat brain membrane homogenates, 1 nM [<sup>3</sup>H]DAMGO as radioligand, IC<sub>50</sub>, half-maximal inhibitory concentration, <sup>2</sup> inhibition of enzymatic hydrolysis of anandamide measured in rat brain membranes, <sup>3</sup> inhibition of enzymatic hydrolysis of arachidonoyl-glycerol measured in cytosolic fraction from COS-7 cells, <sup>4</sup> n/d—not determined.

## 8. Fentanyl-Related MTAs Targeting MOR and σ<sub>1</sub>R

As the last of the ‘second’ targets for fentanyl-based MTAs, we shall discuss the σ<sub>1</sub> receptor (σ<sub>1</sub>R). Despite its name, the σ<sub>1</sub> receptor is not a ‘typical’ receptor, but it is thought to be rather a ‘ligand-operated’ chaperone [85]. σ<sub>1</sub>R stabilizes proteins of endoplasmic reticulum but also regulates (directly or indirectly) ion channels [86], kinases and receptors, including some GPCRs such as the dopamine receptors [87] or μ-opioid receptor [88]. For being involved in many physiological and pathological processes [89,90], σ<sub>1</sub>R was proposed as a therapeutic target for the treatment of inter alia schizophrenia, depression, drug addiction, neurodegenerative diseases or neuropathic pain [91].

As to the latter, it was shown that σ<sub>1</sub>R antagonists do not have antinociceptive action in classical models of acute nociception [92–94], however they inhibit pain in sensitizing pain models [95–98]. Most importantly, σ<sub>1</sub>R antagonists were found to enhance antinociceptive action of classical opioids [99] but without exacerbating their side-effects (tolerance, dependence, constipation) [100]. For these reasons, σ<sub>1</sub>R antagonists were proposed not only as a stand-alone treatment against neuropathic pain but also as adjuvants for opioid therapy [87,100,101].

A closely related idea to combine MOR agonist and σ<sub>1</sub>R antagonist activities in one molecule was probably expressed for the first time in the early 2010s in a few patent applications by ESTEVE Laboratories [102–104]. In the scientific literature, per our knowledge, a first suggestion along these lines was made by Prezzavento et al. [105]. These authors showed that phenazocine enantiomers bind to both MOR and σ<sub>1</sub>R with high affinity and that their antinociceptive action is associated with both these receptors. Hence, they suggested that phenazocine structure might be a scaffold for developing dual MOR agonist/σ<sub>1</sub>R antagonist ligands. In the past very few years (from 2019 onwards) there appeared several papers describing efforts based on the concept of dual MOR/σ<sub>1</sub>R ligands, nicely summarized in a recent review [22].

### 8.1. Affinity of Fentanyl Analogues for $\sigma_1$ R

That fentanyl might be a basis for such dual ligands was one of the conclusions in a 2019 paper of ours [106]. In that study we assayed fentanyl and its 11 commercially available analogues for  $\sigma_1$ R affinity (Figure 9). Our initial interests in the fentanyls' affinities for  $\sigma_1$ R were rather remote from typical medicinal chemistry, but instead we wanted to see if  $\sigma_1$ R affinity could be an important ingredient of fentanyls' secondary pharmacology.

In agreement with the previous reports [107,108], fentanyl (**1.1**) showed a rather low  $\sigma_1$ R affinity with  $K_i = 3718$  nM. Interestingly however, minor structural modifications to the parent structure result in submicromolar affinities. For example, *N*-benzylfentanyl (**8.1**, Figure 9) which is different from the parent by having one methylene unit  $-CH_2-$  less in the **B**-region (*N*-chain), has  $K_i = 240$  nM. *p*-fluorofentanyl (**8.2**) which differs just by having a fluorine atom instead of a hydrogen in the region **C**, exhibits binding with  $K_i = 370$  nM. Similar affinity is found for 3-methylthiofentanyl (**8.3**,  $K_i = 387.78$  nM) that has a methyl group in the piperidine position C3 and a 2-thienyl ring (instead of the phenyl ring) in the *N*-chain (region **B**). The analogues with the 4-axial substitution in the piperidine ring exhibit none or low affinity for  $\sigma_1$ R (**1.4**, **1.5**, **8.7**, **8.8**). Similarly, introduction of a hydroxyl group into the regions **B** or **D** gives compounds without  $\sigma_1$ R affinity (**8.4**, **8.5**, **8.6**).

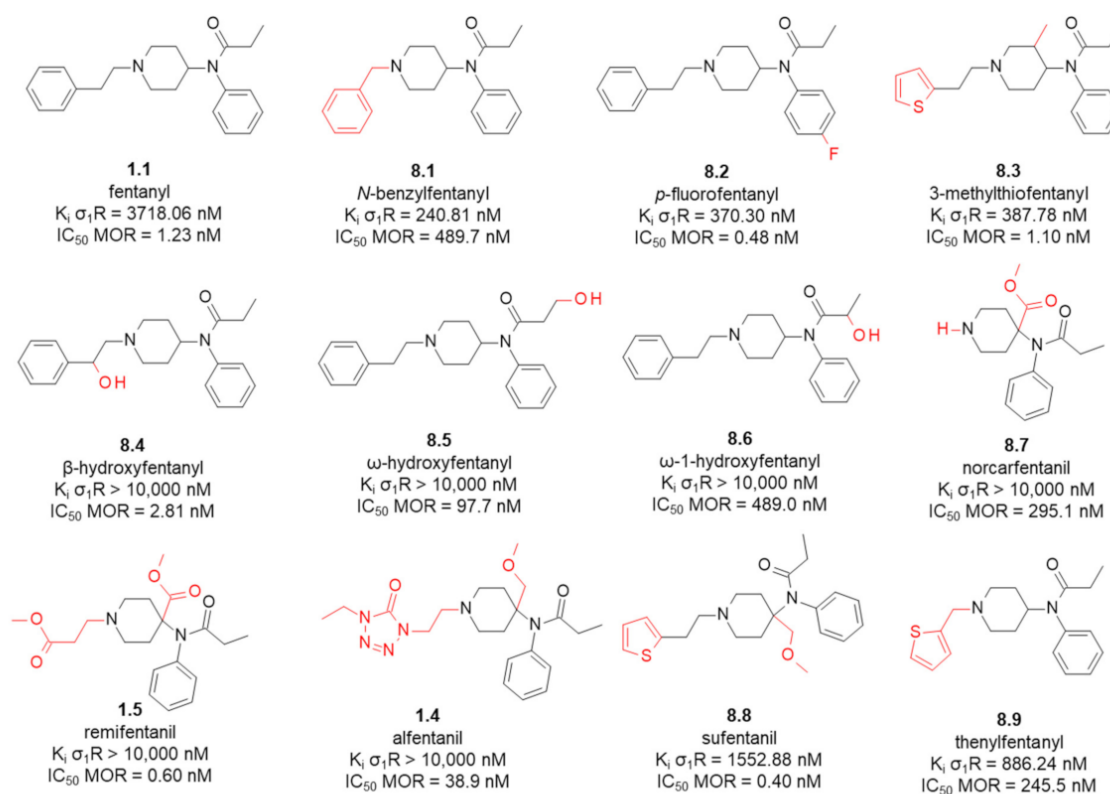


**Figure 9.** MOR and  $\sigma_1$ R affinities of fentanyl and analogues. In red marked are structural differences compared to the parent compound. Data taken from [106] ( $\sigma_1$ R, competitive assays done in guinea pig brain membrane homogenates, [<sup>3</sup>H]-(+)-pentazocine as radioligand) and from [109] (MOR, competitive assays done in rat brain membrane homogenates, 0.5 nM [<sup>3</sup>H]DAMGO as radioligand).

According to modelling of the interactions between  $\sigma_1$ R and selected fentanyls (docking and molecular dynamics), both *N*-benzylfentanyl (**8.1**) and *p*-fluorofentanyl (**8.2**) adopt a binding mode that shares the main features with the binding mode of a high-affinity ligand 4-IBP as found in the 5HK2 crystal structure [110], these being:

- ionic interaction of protonated piperidine's nitrogen with Glu172,
- direction of the anilide's ring towards  $\alpha 4$  and  $\alpha 5$  helices of the receptor,
- positioning of the *N*-substituent towards the bottom of  $\beta$ -barrel (close to Asp126).

Apart from the above mentioned, single ionic interaction, the remaining ligand-receptor contacts seen in the simulations were of apolar character. Based on these computations, we were able to provide reasonable explanations for the rest of the observed affinities.

Comparing the  $\sigma_1$ R binding data to MOR affinities (Figure 9), it is seen that while most of the studied analogues turned out to be MOR-selective, *N*-benzylfentanyl (**8.1**) may be considered a balanced binder to both receptors (or with some minor preference for  $\sigma_1$ R). As such, this very analogue could be a starting point in the search for mixed MOR/ $\sigma_1$ R ligands.

### 8.2. 1-Oxa-4,9-diazaspiro[5.5]undecane Derivatives

A very successful med-chem programme focused on dual  $\mu$ OR agonists/ $\sigma_1$ R antagonists was recently described by García et al. (of ESTEVE Pharmaceuticals SA) [111,112]. In their contributions the team disclosed 1-oxa-4,9-diazaspiro[5.5]undecane (Figure 10) derivatives with the desired dual activity. Although the discovery of these compounds was not directly inspired by fentanyl's structure, some not so remote a similarity between fentanyl (or *N*-benzylfentanyl) and the early structures in this programme (e.g., **8.10** and **8.11**) is obvious to chemist's eyes (Figure 10B). The initial compounds were designed as a result of merging 3D-pharmacophore models of both receptors (based on morphine for  $\mu$ OR and based on a model by Laggner et al. [113] as well as on the in-house SAR data [114] in the case of  $\sigma_1$ R).

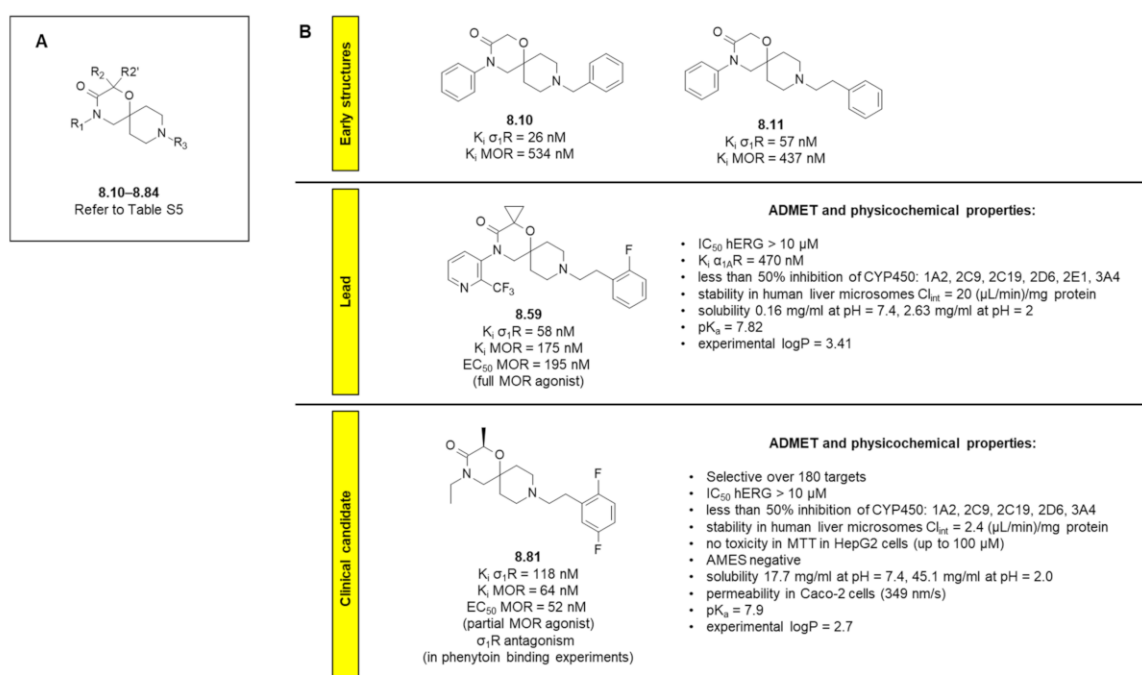


**Figure 10.** (A) General structure of compounds **8.10–8.84**, (B) Structures of key compounds in the programme with some of their pharmacological properties.

Almost 80 analogues (**8.10–8.84**, see Table S5 for structures and affinities) were reported to have been obtained and tested [111,112], out of which about a half exhibited  $K_i < 100$  nM for MOR and about 50 of them showed  $K_i < 100$  nM for  $\sigma_1$ R. Many examples had single-digit nanomolar  $K_i$ 's either for one of the receptors or for both. The issues that were mainly fought with during the SAR exploration was the propensity of these structures to interact with hERG channels and  $\alpha_{1A}$ -adrenergic receptors ( $\alpha_{1A}R$ ; associated with cardiac toxicity). Increasing polarity (decreasing lipophilicity) of the structures was rather unsuccessful in coping with these liabilities, and additionally it gave potency losses at both targets of interest.  $R_2$  substitution with small alkyl groups was very favourable to the binding

at primary targets. The preferred stereochemistry at this position (mainly due to MOR affinity) was *R* (compare for example **8.13** vs. **8.14**, **8.67** vs. **8.68**, **8.81** vs. **8.84**). For the  $R_3$  group, it was established that an arylethyl substituent is required for dual affinity. The later compounds drove structurally away off resembling fentanyl (**8.60–8.84**) [112]. The key step in SAR campaign was elimination of the aryl ring in the 4-position, since in this way it was possible to get rid of  $\alpha_{1A}$ R activity.

Important to note, as the lead compound (**8.59**) [112], the authors chose not the best opioid binder among **8.10–8.59**, but a compound with balanced affinities for the desired targets (MOR  $K_i = 175$  nM,  $\sigma_1$ R  $K_i = 58$  nM). This was justified by the expectation that the best benefit-to-risk ratio would be obtained upon combining  $\sigma_1$ R antagonism with weak/partial MOR agonist: “*efficacy would result from  $\sigma_1$ R antagonism-mediated maximization of modest opioid effect whereas side effects would rely on such nonpotentiated baseline opioid component*” [112].

The lead **8.59** was a full MOR agonist (in vitro), showed moderate  $\alpha_{1A}$ R binding ( $K_i = 470$  nM), no hERG inhibition and selectivity in the selectivity panel. It did also have favourable physicochemical properties and good ADMET data (Figure 10B). In vivo, the compound was shown to be active in acute pain model (mouse paw pressure pain test, ip administration) with  $ED_{50} = 15$  mg/kg, albeit the compound was less potent than the reference oxycodone (per os, po). On the other hand, the authors showed that **8.59** produced less inhibition of the intestinal transit in mice than the reference oxycodone (at equianalgesic doses: 20 mg/kg ip **8.59** vs. 10 mg/kg po oxycodone). Upon intraplantar administration (ipl; 25  $\mu$ g), **8.59** showed local analgesic effect (paw pressure test in mice) which was abolished by a  $\sigma_1$ R agonist PRE-084, that showing a hint in favour of the double mechanism of action.

The lead optimization work eventually resulted in EST73502 (**8.81**, Figure 10B) [112]. This compound turned out to have good and balanced on-target affinities ( $\sigma_1$ R  $K_i = 118$  nM; MOR  $K_i = 64$  nM) and to be very selective (against 180 molecular targets; hERG inhibition  $> 10$   $\mu$ M; low CYP involvement). It did also show favourable physicochemical and ADMET properties (Figure 10B). EST73502 was effective in vivo in the acute pain model (paw pressure test in mice) after oral administration, showing a dose-dependent analgesic effect (64% of MPE) with  $ED_{50} = 14$  mg/kg. The contribution of  $\sigma_1$ R to the analgesic activity of EST73502 was confirmed by the observation that subcutaneous (sc) administration of PRE-084 ( $\sigma_1$ R agonist) diminished the level of antinociceptive effect. The effect was fully abolished with sc administration of MOR antagonist naloxone.

EST73502 (**8.81**) was also tested in vivo in the chronic pain model (partial sciatic nerve ligation in mice) using the von Frey test. The compound (5 mg/kg, ip) was effective over 23 days of the experiment, at the level similar to that produced by oxycodone (1.25 mg/kg, ip). Importantly, contrary to oxycodone, EST73502 (**8.81**) did not produce opiate withdrawal signs (upon administration of naloxone). The dual analgesic showed also less inhibition of the intestinal transit in mice compared to oxycodone (at equianalgesic doses). With all these favourable characteristics, EST73502 (**8.81**) was nominated a clinical candidate. As of 2021, the Phase-I study was announced. Overall, this case demonstrates great potential of the MOR/ $\sigma_1$ R dual ligands concept.

Of note, ESTEVE disclosed also a few sets of dual MOR/ $\sigma_1$ R ligands based on spiroisoquinoline-1,4'-piperidine [115], spiroisoquinoline-4,4'-piperidine [116], amide [117] or piperidinylalkylamide [118] motifs. In some aspects of their structures, all these derivatives bear resemblance to the structure of fentanyl. In particular, many of piperidinylalkylamides in reference [118] are structurally related to *N*-benzylfentanyl (**8.1**, Figure 9).

### 8.3. Amide Derivatives with Piperidine in Their Structures

Xiong et al. successfully designed dual MOR/ $\sigma_1$ R ligands by molecular hybridization. These authors combined (Figure 11) *N*-phenylpropionamide fragment (of fentanyl structure) with the 4-benzylpiperidine (of RC-106 **8.85**, a pan-sigma ligand) [119]. In the works of theirs [119,120], over 60 dual ligands (**8.86–8.147**, Figure 11 and Table S6) were reported to

have been synthesized and tested (Table S6). Around a half of the published examples had  $K_i < 100$  nM for either of the receptors of focus. For nine analogues,  $K_i$  values were below 30 nM for both receptors.

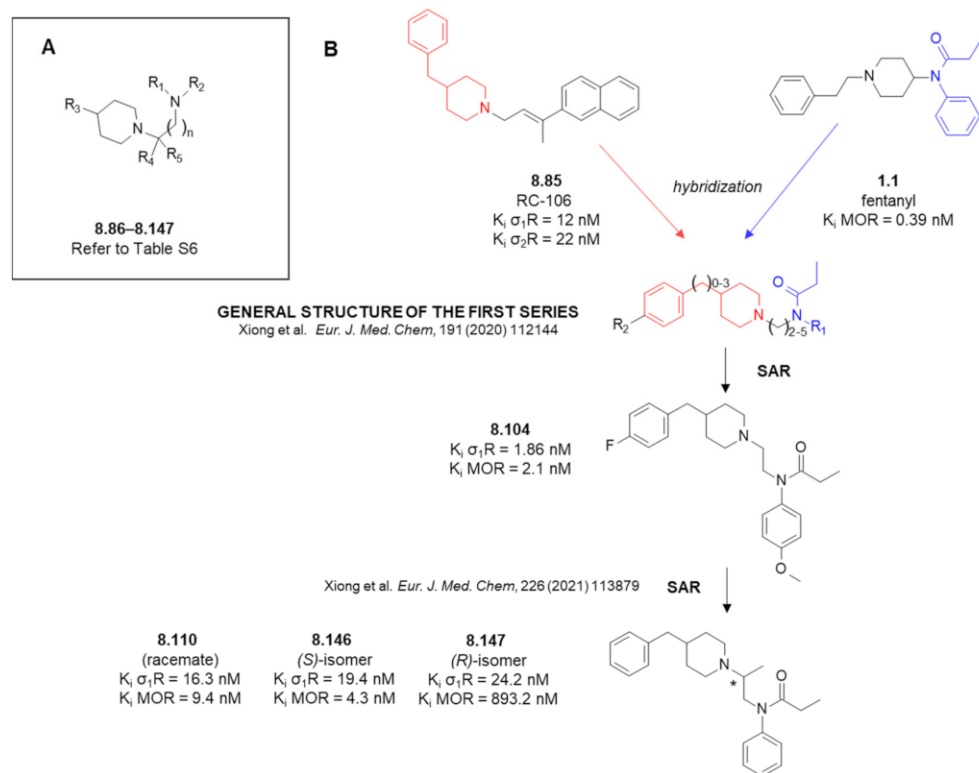


**Figure 11.** (A) General structure of compounds 8.86–8.147. (B) Design principle and key compounds in the programme with some of their pharmacological properties. In red and blue marked are fragments subject to hybridization.

Of the key SAR findings, with respect to  $R_1$  and  $R_2$  groups (Figure 11), the *N*-phenylpropanamide motif (optimally with *para*-fluoro or *para*-methoxy substitution at the ring) is most advantageous for the target affinities. The optimal spacing between the piperidine ring and the amide was afforded by ethylene linker. As to the  $R_3$  group, the best affinities were found for benzyl or substituted benzyl moieties.

Of the first series of analogues [119], compounds **8.104** (Figure 11B) and **8.108** (Table S6) were advanced to more detailed *in vitro* and *in vivo* testing. These compounds were found to be selective against a set of a few receptors ( $\sigma_2R$ , 5-HT<sub>1A</sub>, 5-HT<sub>2A</sub>, histamine H<sub>3</sub> receptor, cannabinoid CB<sub>1</sub> and CB<sub>2</sub> receptors; less than 50% binding at 1  $\mu$ M). Their median lethal doses (**8.104**, LD<sub>50</sub> = 396.7 mg/kg; **8.108**, LD<sub>50</sub> = 415.8 mg/kg; sc injection) were higher than that of a reference  $\sigma_1R$  antagonist (compound S1RA, LD<sub>50</sub> = 357.4 mg/kg, sc). *In vivo*, in the formalin test in mice, both **8.104** and **8.108** were found to exhibit antiallodynic activity (sc pretreatment with 50 mg/kg before formalin injection; half-maximal effective dose, ED<sub>50</sub> for compound **8.104** in Phase II was 15.1 mg/kg). Additionally, this analogue was examined in the chronic constriction injury (CCI) model of neuropathic pain (in rats; von Frey test, day 15 after surgery). Here, 25 mg/kg (sc) of compound **8.104** was found equianalgesic to 50 mg/kg (sc) of S1RA. ED<sub>50</sub> of compound **8.104** was 44.14 mg/kg.

As a result of SAR work around compound **8.104** [120], racemic compounds **8.110** (Figure 11B) and **8.131** (Table S6) were identified as very promising. Enantiomers of **8.110** were synthesized and assayed (**8.146** and **8.147**, Figure 11B). Interestingly, there was a notable stereoselectivity in case of MOR affinity in favour of *S*-configuration (**8.146**), but  $\sigma_1R$  affinities were at a similar level for both isomers. The MOR-agonist/ $\sigma_1R$  antagonist profile of compounds **8.110**, **8.131** and **8.146** was confirmed in functional testing. The

compounds were also found selective (less than 50% binding at 10  $\mu$ M to KOR, DOR,  $\sigma_2$ R, 5-HT<sub>1A</sub>R, 5-HT<sub>2A</sub>R, H<sub>3</sub>R, serotonin transporter and noradrenaline transporter) and safe (acute toxicity after sc injection; the best LD<sub>50</sub> = 271.6 mg/kg found for **8.146**).

The compound **8.146** was also found to be an effective analgesic in mice in the acetic acid-induced writhing test (ED<sub>50</sub> = 0.47 mg/kg) and in the formalin test (acute and chronic pain; ED<sub>50</sub> = 0.32 mg/kg). In the latter test, 1 mg/kg (sc) of **8.146** was similarly effective in Phase I to the maximally effective dose of 0.05 mg/kg fentanyl (sc). In the hot-plate test, 3 mg/kg **8.146** (sc) was equianalgesic to fentanyl 0.1 mg/kg (sc) while ED<sub>50</sub> was found to be 1.0 mg/kg. In the Von Frey test (neuropathic pain CCI-model) 0.3 mg/kg was equianalgesic to 0.05 mg/kg of fentanyl and its ED<sub>50</sub> = 0.48 mg/kg.

Compound **8.146** was also investigated as to the typical opioid-side effects and compared to fentanyl (sc injections at equianalgesic doses of 1 mg/kg and 0.05 mg/kg, for **8.146** and fentanyl, respectively). It was found that **8.146** did not produce conditioned place preference, did not depress the respiratory rate (whole body plethysmography), did not induce physical dependence (naloxone-induced withdrawal) and did not have any significant effect on exploratory locomotor activity. On the contrary, fentanyl showed all these undesired characteristics despite a much lower dose. Additionally, favourable pharmacokinetic properties of Compound **8.146** were found after 1 mg/kg sc administration ( $t_{1/2}$  = 1.71 h,  $T_{max}$  = 0.25h,  $C_{max}$  = 214 ng/mL). Given all these favourable properties, the compound **8.146** was described as a potential candidate drug for treating neuropathic pain, with further studies of this compound heralded.

#### 8.4. Remark on $\sigma_2$ R

Let us add here that a direction worth examination is if fentanyl-based compounds could bind another  $\sigma$ -binding site, the  $\sigma_2$  receptor ( $\sigma_2$ R, transmembrane protein 9, TMEM97 [121]). It seems probable that they do, since many  $\sigma_1$ R ligands have appreciable affinity for  $\sigma_2$ R, too. There is also a prediction from a QSAR model based a large dataset of  $\sigma_2$ R ligands that fentanyl would bind  $\sigma_2$ R with  $K_i$  in middle nanomolar range [122]. If confirmed, this could hypothetically open way to mixed opioid/ $\sigma_2$ R ligands utilizing the fentanyl scaffold. Application of  $\sigma_2$ R ligands in the therapy of cancers and neurological, inflammatory and autoimmune disease has been proposed [123].

## 9. Outlook

Opioid/non-opioid multitarget analgesics are a promising approach towards obtaining more effective and safer drugs against pain, including chronic pain with neuropathic components. A key consideration in search for MTAs is the choice of pharmacophores to be used and of the manner in which they are brought together in one molecule. In this review we discussed the attempts to create opioid/non-opioid MTAs that utilized fentanyl structural elements as opioid pharmacophores.

In most of the considered cases, the auxiliary pharmacophores were introduced by fusing both parts 'side-to-side' or by separating them by the means of a linker. While conceptually simple, such approaches are rarely successful with just one 'shot'. The structure of fentanyl is rather compact and non-redundant and any replacements or deletions may lead to deterioration or ablation of opioid activity. At the same time, it is not easy to introduce the second type activity into the structure. Moreover, structural optimization is difficult due to the fact that MOR affinity trends can be antiparallel to those of the auxiliary target. Intriguingly, even if opioid affinity is preserved (at least to some extent), not necessarily follows the functional activity and even inversion of function (agonist into antagonist) can occur.

Which further directions are worth exploration? In none of the 'fusing' or 'linking' attempts were employed the structural modifications known to improve MOR affinity of fentanyls, e.g.,  $\alpha$ -methyl,  $\beta$ -hydroxyl, 3-methyl, 4-methoxymethyl, 4-carboxymethyl etc. In particular, the two latter substitutions deserve examination in MTAs, since they are known to produce very potent MOR ligands. On the other hand, it cannot be guaranteed that these

substitutions would be compatible with the requirements of the auxiliary molecular target. For example, it seems that 4-axial substitution at the piperidine ring negatively affects  $\sigma_1$ R binding [106]. A certain problem with 4-axial substituted fentanyl analogues is that they require multi-step and rather low-yielding syntheses. Notably however, some progress in their syntheses have been reported in several past years [124–127]. Moreover, in the field of mixed opioid ligands, there is an interesting recent example, in which carfentanil (**1.2**) fragments were hybridized with peptide dermorphine analogues to yield potent analgesics with improved properties [128].

Yet other direction that have not been tried so far is attaching the linker directly to the piperidine ring (e.g., in positions 3 or axial 4 in region **A**) without removal or modification of the remaining fentanyl elements. This is likely to be synthetically demanding but several valuable strategies that might enable it have been described [129–131].

Future attempts should also benefit from applying molecular modelling and structure-based approaches. Recent years have witnessed major progress in GPCR structural biology. This has enabled wider application of structure-based approaches in GPCR ligand discovery [132,133]. For the design of MTAs, it is vital that four MOR structures (Table S7) are now available in the PDB database [134–136]. Of particular importance, interactions of fentanyl with MOR were subject of several recent studies that used docking, molecular dynamics and other modelling techniques [109,137–143]. A useful tool for interpretation of MOR ligands' SAR, based on template alignment, modelling have been devised, too [144]. It is also for many non-opioid GPCRs related to pain (including those discussed in this paper) that the structures have been recently solved (Table S8, refer to the GPCRdb service for an up-to-date and comprehensive list [145]). Of late, structural insights have become available also for binding of ligands to the  $\sigma$ -receptors [110,146,147] (Table S9) All these, along with extensive SAR data gathered over the years, might be expected to expedite opioid/non-opioid MTAs' design.

**Supplementary Materials:** Supplementary materials can be found at <https://www.mdpi.com/article/10.3390/ijms23052766/s1>. References [148–168] are cited in the supplementary materials.

**Funding:** Piotr F.J. Lipiński acknowledges the institutional grant at Mossakowski Medical Research Institute PAS (grant no. FBW-010).

**Conflicts of Interest:** The authors declare no conflict of interest.

## References

1. Benyamin, R.; Trescot, A.M.; Datta, S.; Buenaventura, R.; Adlaka, R.; Sehgal, N.; Glaser, S.E.; Vallejo, R. Opioid complications and side effects. *Pain Physician* **2008**, *11*, S105–S120. [[CrossRef](#)] [[PubMed](#)]
2. de Vries, F.; Bruin, M.; Lobatto, D.J.; Dekkers, O.M.; Schoones, J.W.; van Furth, W.R.; Pereira, A.M.; Karavitaki, N.; Biermasz, N.R.; Zamanipour Najafabadi, A.H. Opioids and Their Endocrine Effects: A Systematic Review and Meta-analysis. *J. Clin. Endocrinol. Metab.* **2020**, *105*, 1020–1029. [[CrossRef](#)] [[PubMed](#)]
3. Hayhurst, C.J.; Durieux, M.E. Differential Opioid Tolerance and Opioid-induced Hyperalgesia. *Anesthesiology* **2016**, *124*, 483–488. [[CrossRef](#)] [[PubMed](#)]
4. Colloca, L.; Ludman, T.; Bouhassira, D.; Baron, R.; Dickenson, A.H.; Yarnitsky, D.; Freeman, R.; Truini, A.; Attal, N.; Finnerup, N.B.; et al. Neuropathic pain. *Nat. Rev. Dis. Prim.* **2017**, *3*, 17002. [[CrossRef](#)] [[PubMed](#)]
5. Machelska, H.; Celik, M.Ö. Advances in Achieving Opioid Analgesia Without Side Effects. *Front. Pharmacol.* **2018**, *9*, 1388. [[CrossRef](#)]
6. Dvoracko, S.; Stefanucci, A.; Novellino, E.; Mollica, A. The design of multitarget ligands for chronic and neuropathic pain. *Future Med. Chem.* **2015**, *7*, 2469–2483. [[CrossRef](#)] [[PubMed](#)]
7. Turnaturi, R.; Aricò, G.; Ronsisvalle, G.; Parenti, C.; Pasquinucci, L. Multitarget opioid ligands in pain relief: New players in an old game. *Eur. J. Med. Chem.* **2016**, *108*, 211–228. [[CrossRef](#)] [[PubMed](#)]
8. Zhang, L.; Zhang, J.-T.; Hang, L.; Liu, T. Mu Opioid Receptor Heterodimers Emerge as Novel Therapeutic Targets: Recent Progress and Future Perspective. *Front. Pharmacol.* **2020**, *11*, 1078. [[CrossRef](#)] [[PubMed](#)]
9. Starnowska-Sokół, J.; Przewłocka, B. Multifunctional Opioid-Derived Hybrids in Neuropathic Pain: Preclinical Evidence, Ideas and Challenges Joanna. *Molecules* **2020**, *25*, 5520. [[CrossRef](#)]

10. Mollica, A.; Pelliccia, S.; Famiglini, V.; Stefanucci, A.; Macedonio, G.; Chiavaroli, A.; Orlando, G.; Brunetti, L.; Ferrante, C.; Pieretti, S.; et al. Exploring the first Rimonabant analog-opioid peptide hybrid compound, as bivalent ligand for CB1 and opioid receptors. *J. Enzyme Inhib. Med. Chem.* **2017**, *32*, 444–451. [[CrossRef](#)] [[PubMed](#)]
11. Le Naour, M.; Akgün, E.; Yekkirala, A.; Lunzer, M.M.; Powers, M.D.; Kalyuzhny, A.E.; Portoghese, P.S. Bivalent Ligands That Target  $\mu$  Opioid (MOP) and Cannabinoid1 (CB 1) Receptors Are Potent Analgesics Devoid of Tolerance. *J. Med. Chem.* **2013**, *56*, 5505–5513. [[CrossRef](#)]
12. Kleczkowska, P.; Nowicka, K.; Bujalska-Zadrozny, M.; Hermans, E. Neurokinin-1 receptor-based bivalent drugs in pain management: The journey to nowhere? *Pharmacol. Ther.* **2019**, *196*, 44–58. [[CrossRef](#)]
13. Dyniewicz, J.; Lipiński, P.F.J.; Kosson, P.; Bochyńska-Czyż, M.; Matalińska, J.; Misicka, A. Antinociceptive and Cytotoxic Activity of Opioid Peptides with Hydrazone and Hydrazide Moieties at the C-Terminus. *Molecules* **2020**, *25*, 3429. [[CrossRef](#)]
14. Lee, Y.S.; Agnes, R.S.; Davis, P.; Ma, S.; Badghisi, H.; Lai, J.; Porreca, F.; Hruby, V.J. Partial Retro–Inverso, Retro, and Inverso Modifications of Hydrazide Linked Bifunctional Peptides for Opioid and Cholecystokinin (CCK) Receptors. *J. Med. Chem.* **2007**, *50*, 165–168. [[CrossRef](#)]
15. Agnes, R.S.; Lee, Y.S.; Davis, P.; Ma, S.; Badghisi, H.; Porreca, F.; Lai, J.; Hruby, V.J. Structure–Activity Relationships of Bifunctional Peptides Based on Overlapping Pharmacophores at Opioid and Cholecystokinin Receptors. *J. Med. Chem.* **2006**, *49*, 2868–2875. [[CrossRef](#)] [[PubMed](#)]
16. Kleczkowska, P.; Kosson, P.; Ballet, S.; Van den Eynde, I.; Tsuda, Y.; Tourwé, D.; Lipkowski, A.W. PK20, a New Opioid-Neurotensin Hybrid Peptide That Exhibits Central and Peripheral Antinociceptive Effects. *Mol. Pain* **2010**, *6*, 86. [[CrossRef](#)]
17. Gonzalez, S.; Dumitrascuta, M.; Eiselt, E.; Louis, S.; Kunze, L.; Blasiol, A.; Vivancos, M.; Previti, S.; Dewolf, E.; Martin, C.; et al. Optimized Opioid-Neurotensin Multitarget Peptides: From Design to Structure-Activity Relationship Studies. *J. Med. Chem.* **2020**, *63*, 12929–12941. [[CrossRef](#)] [[PubMed](#)]
18. Starnowska-Sokół, J.; Piotrowska, A.; Bogacka, J.; Makuch, W.; Mika, J.; Witkowska, E.; Godlewska, M.; Osiejuk, J.; Gałarz, S.; Misicka, A.; et al. Novel hybrid compounds, opioid agonist+melanocortin 4 receptor antagonist, as efficient analgesics in mouse chronic constriction injury model of neuropathic pain. *Neuropharmacology* **2020**, *178*, 108232. [[CrossRef](#)]
19. Witkowska, E.; Godlewska, M.; Osiejuk, J.; Gałarz, S.; Wileńska, B.; Kosińska, K.; Starnowska-Sokół, J.; Piotrowska, A.; Lipiński, P.F.J.; Matalińska, J.; et al. Bifunctional Opioid/Melanocortin Peptidomimetics for Use in Neuropathic Pain: Variation in the Type and Length of the Linker Connecting the Two Pharmacophores. *Int. J. Mol. Sci.* **2022**, *23*, 674. [[CrossRef](#)] [[PubMed](#)]
20. Wang, Z.-L.L.; Pan, J.-X.X.; Song, J.-J.J.; Tang, H.-H.H.; Yu, H.-P.P.; Li, X.-H.H.; Li, N.; Zhang, T.; Zhang, R.; Zhang, M.-N.N.; et al. Structure-Based Optimization of Multifunctional Agonists for Opioid and Neuropeptide FF Receptors with Potent Nontolerance Forming Analgesic Activities. *J. Med. Chem.* **2016**, *59*, 10198–10208. [[CrossRef](#)]
21. Vardanyan, R.S.; Hruby, V.J. Substituted 1-Arylalkyl-4-Acylaminopiperidine Compounds and Methods of Producing and Using the Same. WO2017034631A1, 24 August 2015.
22. Zhuang, T.; Xiong, J.; Hao, S.; Du, W.; Liu, Z.; Liu, B.; Zhang, G.; Chen, Y. Bifunctional  $\mu$  opioid and  $\sigma$ 1 receptor ligands as novel analgesics with reduced side effects. *Eur. J. Med. Chem.* **2021**, *223*, 113658. [[CrossRef](#)]
23. Vardanyan, R.; Vijay, G.; Nichol, G.S.; Liu, L.; Kumarasinghe, I.; Davis, P.; Vanderah, T.; Porreca, F.; Lai, J.; Hruby, V.J. Synthesis and investigations of double-pharmacophore ligands for treatment of chronic and neuropathic pain. *Bioorg. Med. Chem.* **2009**, *17*, 5044–5053. [[CrossRef](#)]
24. Monti, L.; Stefanucci, A.; Pieretti, S.; Marzoli, F.; Fidanza, L.; Mollica, A.; Mirzaie, S.; Carradori, S.; De Petrocellis, L.; Schiano Moriello, A.; et al. Evaluation of the analgesic effect of 4-anilidopiperidine scaffold containing ureas and carbamates. *J. Enzyme Inhib. Med. Chem.* **2016**, *31*, 1638–1647. [[CrossRef](#)]
25. Mollica, A.; Costante, R.; Novellino, E.; Stefanucci, A.; Pieretti, S.; Zador, F.; Samavati, R.; Borsodi, A.; Benyhe, S.; Vetter, I.; et al. Design, Synthesis and Biological Evaluation of Two Opioid Agonist and Ca v 2.2 Blocker Multitarget Ligands. *Chem. Biol. Drug Des.* **2015**, *86*, 156–162. [[CrossRef](#)]
26. Montero, A.; Goya, P.; Jagerovic, N.; Callado, L.F.; Meana, J.J.; Girón, R.; Goicoechea, C.; Martín, M.I. Guanidinium and aminoimidazolium derivatives of N-(4-piperidyl)propanamides as potential ligands for  $\mu$  opioid and I2-imidazoline receptors: Synthesis and pharmacological screening. *Bioorg. Med. Chem.* **2002**, *10*, 1009–1018. [[CrossRef](#)]
27. Dardonville, C.; Jagerovic, N.; Callado, L.F.; Meana, J.J. Fentanyl derivatives bearing aliphatic alkaneguanidinium moieties: A new series of hybrid molecules with significant binding affinity for  $\mu$ -opioid receptors and I2-imidazoline binding sites. *Bioorg. Med. Chem. Lett.* **2004**, *14*, 491–493. [[CrossRef](#)] [[PubMed](#)]
28. Dardonville, C.; Fernandez-Fernandez, C.; Gibbons, S.-L.; Ryan, G.J.; Jagerovic, N.; Gabilondo, A.M.; Meana, J.J.; Callado, L.F. Synthesis and pharmacological studies of new hybrid derivatives of fentanyl active at the  $\mu$ -opioid receptor and I2-imidazoline binding sites. *Bioorg. Med. Chem.* **2006**, *14*, 6570–6580. [[CrossRef](#)] [[PubMed](#)]
29. Morphy, R.; Rankovic, Z. Designed multiple ligands. An emerging drug discovery paradigm. *J. Med. Chem.* **2005**, *48*, 6523–6543. [[CrossRef](#)]
30. Pawełczyk, A.; Sowa-Kasprzak, K.; Olender, D.; Zaprutko, L. Molecular Consortia—Various Structural and Synthetic Concepts for More Effective Therapeutics Synthesis. *Int. J. Mol. Sci.* **2018**, *19*, 1104. [[CrossRef](#)]
31. Burns, S.M.; Cunningham, C.W.; Mercer, S.L. DARK Classics in Chemical Neuroscience: Fentanyl. *ACS Chem. Neurosci.* **2018**, *9*, 2428–2437. [[CrossRef](#)]
32. Clotz, M.A.; Nahata, M.C. Clinical uses of fentanyl, sufentanil, and alfentanil. *Clin. Pharm.* **1991**, *10*, 581–593. [[CrossRef](#)] [[PubMed](#)]

33. Jannetto, P.J.; Helander, A.; Garg, U.; Janis, G.C.; Goldberger, B.; Ketha, H. The Fentanyl Epidemic and Evolution of Fentanyl Analogs in the United States and the European Union. *Clin. Chem.* **2019**, *65*, 242–253. [[CrossRef](#)] [[PubMed](#)]
34. Valdez, C.A.; Leif, R.N.; Mayer, B.P. An Efficient, Optimized Synthesis of Fentanyl and Related Analogs. *PLoS ONE* **2014**, *9*, e108250. [[CrossRef](#)] [[PubMed](#)]
35. Janssen, P.A.J.; Gardocki, J.F. Method for Producing Analgesia. U.S. Patent 3141823, 21 July 1964.
36. Janssen, P.A.J. 1-Aralkyl-4-(N-Aryl-Carbonyl Amino)-Piperidines and Related Compounds. U.S. Patent 3164600, 5 January 1965.
37. Vardanyan, R.S.; Hruby, V.J. Fentanyl-related compounds and derivatives: Current status and future prospects for pharmaceutical applications. *Future Med. Chem.* **2014**, *6*, 385–412. [[CrossRef](#)] [[PubMed](#)]
38. Ringuette, A.E.; Spock, M.; Lindsley, C.W.; Bender, A.M. DARK Classics in Chemical Neuroscience: Carfentanil. *ACS Chem. Neurosci.* **2020**, *11*, 3955–3967. [[CrossRef](#)]
39. Wang, Z.-X.; Zhu, Y.-C.; Jin, W.-Q.; Chen, X.-J.; Chen, J.; Ji, R.-Y.; Chi, Z.-Q. Stereoisomers of N-[1-(2-Hydroxy-2-phenylethyl)-3-methyl-4-piperidyl]-N-phenylpropanamide: Synthesis, Stereochemistry, Analgesic Activity, and Opioid Receptor Binding Characteristics. *J. Med. Chem.* **1995**, *38*, 3652–3659. [[CrossRef](#)]
40. Janssens, F.; Torremans, J.; Janssen, P.A.J. Synthetic 1,4-disubstituted 1,4-dihydro-5H-tetrazol-5-one derivatives of fentanyl: Alfentanil (R 39209), a potent, extremely short-acting narcotic analgesic. *J. Med. Chem.* **1986**, *29*, 2290–2297. [[CrossRef](#)]
41. Feldman, P.L.; James, M.K.; Brackeen, M.F.; Bilotta, J.M.; Schuster, S.V.; Lahey, A.P.; Lutz, M.W.; Johnson, M.R.; Leighton, H.J. Design, synthesis, and pharmacological evaluation of ultrashort- to long-acting opioid analgesics. *J. Med. Chem.* **1991**, *34*, 2202–2208. [[CrossRef](#)]
42. Regunathan, S.; Reis, D.J. Imidazoline Receptors and Their Endogenous Ligands. *Annu. Rev. Pharmacol. Toxicol.* **1996**, *36*, 511–544. [[CrossRef](#)]
43. Li, J.-X. Imidazoline I2 receptors: An update. *Pharmacol. Ther.* **2017**, *178*, 48–56. [[CrossRef](#)]
44. Kimura, A.; Tyacke, R.J.; Robinson, J.J.; Husbands, S.M.; Minchin, M.C.W.; Nutt, D.J.; Hudson, A.L. Identification of an imidazoline binding protein: Creatine kinase and an imidazoline-2 binding site. *Brain Res.* **2009**, *1279*, 21–28. [[CrossRef](#)] [[PubMed](#)]
45. Bousquet, P.; Hudson, A.; García-Sevilla, J.A.; Li, J.-X. Imidazoline Receptor System: The Past, the Present, and the Future. *Pharmacol. Rev.* **2020**, *72*, 50–79. [[CrossRef](#)]
46. Li, J.-X.; Zhang, Y. Imidazoline I2 receptors: Target for new analgesics? *Eur. J. Pharmacol.* **2011**, *658*, 49–56. [[CrossRef](#)] [[PubMed](#)]
47. Rovati, L.C.; Brambilla, N.; Blicharski, T.; Connell, J.; Vitalini, C.; Bonazzi, A.; Giacobelli, G.; Girolami, F.; D’Amato, M. Efficacy and safety of the first-in-class imidazoline-2 receptor ligand CR4056 in pain from knee osteoarthritis and disease phenotypes: A randomized, double-blind, placebo-controlled phase 2 trial. *Osteoarthr. Cartil.* **2020**, *28*, 22–30. [[CrossRef](#)] [[PubMed](#)]
48. Martin-Gomez, J.I.; Ruiz, J.; Callado, L.F.; Garibi, J.M.; Aguinaco, L.; Barturen, F.; Meana, J.J. Increased density of I2-imidazoline receptors in human glioblastomas. *Neuroreport* **1996**, *7*, 1393–1396. [[CrossRef](#)] [[PubMed](#)]
49. Weltrowska, G.; Chung, N.N.; Lemieux, C.; Guo, J.; Lu, Y.; Wilkes, B.C.; Schiller, P.W. “Carba”-Analogues of Fentanyl are Opioid Receptor Agonists. *J. Med. Chem.* **2010**, *53*, 2875–2881. [[CrossRef](#)]
50. Jagerovic, N.; Fernández-Fernández, C.; Erdozain, A.M.; Girón, R.; Sánchez, E.; López-Moreno, J.A.; Morales, P.; Rodríguez de Fonseca, F.; Goya, P.; Meana, J.J.; et al. Combining rimonabant and fentanyl in a single entity: Preparation and pharmacological results. *Drug Des. Devel. Ther.* **2014**, *8*, 263–277. [[CrossRef](#)]
51. Zádor, F.; Wollemann, M. Receptome: Interactions between three pain-related receptors or the “Triumvirate” of cannabinoid, opioid and TRPV1 receptors. *Pharmacol. Res.* **2015**, *102*, 254–263. [[CrossRef](#)]
52. Trang, T.; Sutak, M.; Jhamandas, K. Involvement of cannabinoid (CB1)-receptors in the development and maintenance of opioid tolerance. *Neuroscience* **2007**, *146*, 1275–1288. [[CrossRef](#)]
53. Dvoráckó, S.; Keresztes, A.; Mollica, A.; Stefanucci, A.; Macedonio, G.; Pieretti, S.; Zádor, F.; Walter, F.R.; Deli, M.A.; Kékesi, G.; et al. Preparation of bivalent agonists for targeting the mu opioid and cannabinoid receptors. *Eur. J. Med. Chem.* **2019**, *178*, 571–588. [[CrossRef](#)] [[PubMed](#)]
54. Seely, K.A.; Brents, L.K.; Franks, L.N.; Rajasekaran, M.; Zimmerman, S.M.; Fantegrossi, W.E.; Prather, P.L. AM-251 and rimonabant act as direct antagonists at mu-opioid receptors: Implications for opioid/cannabinoid interaction studies. *Neuropharmacology* **2012**, *63*, 905–915. [[CrossRef](#)]
55. Zádor, F.; Ötvös, F.; Benyhe, S.; Zimmer, A.; Páldy, E. Inhibition of forebrain  $\mu$ -opioid receptor signaling by low concentrations of rimonabant does not require cannabinoid receptors and directly involves  $\mu$ -opioid receptors. *Neurochem. Int.* **2012**, *61*, 378–388. [[CrossRef](#)] [[PubMed](#)]
56. Zádor, F.; Kocsis, D.; Borsodi, A.; Benyhe, S. Micromolar concentrations of rimonabant directly inhibits delta opioid receptor specific ligand binding and agonist-induced G-protein activity. *Neurochem. Int.* **2014**, *67*, 14–22. [[CrossRef](#)] [[PubMed](#)]
57. Serra, S.; Carai, M.A.; Brunetti, G.; Gomez, R.; Melis, S.; Vacca, G.; Colombo, G.; Gessa, G.L. The cannabinoid receptor antagonist SR 141716 prevents acquisition of drinking behavior in alcohol-preferring rats. *Eur. J. Pharmacol.* **2001**, *430*, 369–371. [[CrossRef](#)]
58. Bagley, J.R.; Wynn, R.L.; Rudo, F.G.; Doorley, B.M.; Spencer, H.K.; Spaulding, T. New 4-(heteroanilido)piperidines, structurally related to the pure opioidagonist fentanyl, with agonist and/or antagonist properties. *J. Med. Chem.* **1989**, *32*, 663–671. [[CrossRef](#)]
59. Qin, Y.; Ni, L.; Shi, J.; Zhu, Z.; Shi, S.; Lam, A.; Magiera, J.; Sekar, S.; Kuo, A.; Smith, M.T.; et al. Synthesis and Biological Evaluation of Fentanyl Analogues Modified at Phenyl Groups with Alkyls. *ACS Chem. Neurosci.* **2019**, *10*, 201–208. [[CrossRef](#)] [[PubMed](#)]
60. Zubrzycka, M.; Janecka, A. Substance P: Transmitter of nociception (Minireview). *Endocr. Regul.* **2000**, *34*, 195–201.

61. Xiao, J.; Zeng, S.; Wang, X.; Babazada, H.; Li, Z.; Liu, R.; Yu, W. Neurokinin 1 and opioid receptors: Relationships and interactions in nervous system. *Transl. Perioper. Pain Med.* **2016**, *1*, 11–21. [PubMed]
62. Ossipov, M.H.; Lai, J.; King, T.; Vanderah, T.W.; Porreca, F. Underlying mechanisms of pronociceptive consequences of prolonged morphine exposure. *Biopolymers* **2005**, *80*, 319–324. [CrossRef] [PubMed]
63. Powell, K.J.; Quirion, R.; Jhamandas, K. Inhibition of neurokinin-1-substance P receptor and prostanoid activity prevents and reverses the development of morphine tolerance in vivo and the morphine-induced increase in CGRP expression in cultured dorsal root ganglion neurons. *Eur. J. Neurosci.* **2003**, *18*, 1572–1583. [CrossRef] [PubMed]
64. Cream, R.M.; Kato, T.; Shimonaka, H.; Marchand, J.E.; Wurm, W.H. Substance P markedly potentiates the antinociceptive effects of morphine sulfate administered at the spinal level. *Proc. Natl. Acad. Sci. USA* **1993**, *90*, 3564–3568. [CrossRef] [PubMed]
65. Vardanyan, R.; Kumirov, V.K.; Nichol, G.S.; Davis, P.; Liktor-Busa, E.; Rankin, D.; Varga, E.; Vanderah, T.; Porreca, F.; Lai, J.; et al. Synthesis and biological evaluation of new opioid agonist and neurokinin-1 antagonist bivalent ligands. *Bioorg. Med. Chem.* **2011**, *19*, 6135–6142. [CrossRef] [PubMed]
66. MacLeod, A.M.; Merchant, K.J.; Brookfield, F.; Kelleher, F.; Stevenson, G.; Owens, A.P.; Swain, C.J.; Cascieri, M.A.; Sadowski, S. Identification of L-Tryptophan Derivatives with Potent and Selective Antagonist Activity at the NK1 Receptor. *J. Med. Chem.* **1994**, *37*, 1269–1274. [CrossRef]
67. Ambrose, L.M.; Unterwald, E.M.; Van Bockstaele, E.J. Ultrastructural evidence for co-localization of dopamine D2 and  $\mu$ -opioid receptors in the rat dorsolateral striatum. *Anat. Rec.* **2004**, *279A*, 583–591. [CrossRef]
68. Qian, M.; Vasudevan, L.; Huysentruyt, J.; Risseuw, M.D.P.; Stove, C.; Vanderheyden, P.M.L.; Van Craenenbroeck, K.; Van Calenbergh, S. Design, Synthesis, and Biological Evaluation of Bivalent Ligands Targeting Dopamine D2 -Like Receptors and the  $\mu$ -Opioid Receptor. *ChemMedChem* **2018**, *13*, 944–956. [CrossRef] [PubMed]
69. Weber, S.C.; Beck-Schimmer, B.; Kajdi, M.-E.; Müller, D.; Tobler, P.N.; Quednow, B.B. Dopamine D2/3- and  $\mu$ -opioid receptor antagonists reduce cue-induced responding and reward impulsivity in humans. *Transl. Psychiatry* **2016**, *6*, e850. [CrossRef] [PubMed]
70. Kumar, V.; Bonifazi, A.; Ellenberger, M.P.; Keck, T.M.; Pommier, E.; Rais, R.; Slusher, B.S.; Gardner, E.; You, Z.-B.; Xi, Z.-X.; et al. Highly Selective Dopamine D3 Receptor (D3R) Antagonists and Partial Agonists Based on Eticlopride and the D3R Crystal Structure: New Leads for Opioid Dependence Treatment. *J. Med. Chem.* **2016**, *59*, 7634–7650. [CrossRef]
71. Gago, B.; Suárez-Boomgaard, D.; Fuxe, K.; Brené, S.; Reina-Sánchez, M.D.; Rodríguez-Pérez, L.M.; Agnati, L.F.; de la Calle, A.; Rivera, A. Effect of acute and continuous morphine treatment on transcription factor expression in subregions of the rat caudate putamen. Marked modulation by D4 receptor activation. *Brain Res.* **2011**, *1407*, 47–61. [CrossRef] [PubMed]
72. Gago, B.; Fuxe, K.; Agnati, L.; Peñafiel, A.; De La Calle, A.; Rivera, A. Dopamine D4 receptor activation decreases the expression of  $\mu$ -opioid receptors in the rat striatum. *J. Comp. Neurol.* **2007**, *502*, 358–366. [CrossRef] [PubMed]
73. Hagelberg, N.; Kajander, J.K.; Nägren, K.; Hinkka, S.; Hietala, J.; Scheinin, H.  $\mu$ -Receptor agonism with alfentanil increases striatal dopamine D2 receptor binding in man. *Synapse* **2002**, *45*, 25–30. [CrossRef]
74. Park, Y.; Kang Ho, I.; Fan, L.-W.; Loh, H.H.; Ko, K.H. Region specific increase of dopamine receptor D1/D2 mRNA expression in the brain of  $\mu$ -opioid receptor knockout mice. *Brain Res.* **2001**, *894*, 311–315. [CrossRef]
75. Bonifazi, A.; Battiti, F.O.; Sanchez, J.; Zaidi, S.A.; Bow, E.; Makarova, M.; Cao, J.; Shaik, A.B.; Sulima, A.; Rice, K.C.; et al. Novel Dual-Target  $\mu$ -Opioid Receptor and Dopamine D3 Receptor Ligands as Potential Nonaddictive Pharmacotherapeutics for Pain Management. *J. Med. Chem.* **2021**, *64*, 7778–7808. [CrossRef] [PubMed]
76. Jevtic, I.; Penjisevic, J.; Ivanovic, M.; Kostic-Rajacic, S. Synthetic route towards potential bivalent ligands possessing opioid and D2/D3 pharmacophores. *J. Serbian Chem. Soc.* **2019**, *84*, 639–647. [CrossRef]
77. Jevtic, I.; Penjisevic, J.; Savic-Vujovic, K.; Srebro, D.; Vuckovic, S.; Ivanovic, M.; Kostic-Rajacic, S.  $\mu$ -opioid/D2 dopamine receptor pharmacophore containing ligands: Synthesis and pharmacological evaluation. *J. Serbian Chem. Soc.* **2020**, *85*, 711–720. [CrossRef]
78. Jevtić, I. Synthesis, Pharmacological Evaluation and Docking Analysis of Novel Anilidopiperidines (in Serbian). Ph.D. Thesis, University of Belgrade, Belgrade, Serbia, 2020. Available online: <https://nardus.mpn.gov.rs/handle/123456789/17614> (accessed on 11 December 2020).
79. Varrassi, G.; Yeam, C.T.; Rekatsina, M.; Pergolizzi, J.V.; Zis, P.; Paladini, A. The Expanding Role of the COX Inhibitor/Opioid Receptor Agonist Combination in the Management of Pain. *Drugs* **2020**, *80*, 1443–1453. [CrossRef] [PubMed]
80. Petrosino, S.; Di Marzo, V. FAAH and MAGL inhibitors: Therapeutic opportunities from regulating endocannabinoid levels. *Curr. Opin. Investig. Drugs* **2010**, *11*, 51–62. [PubMed]
81. Pertwee, R.G. Elevating endocannabinoid levels: Pharmacological strategies and potential therapeutic applications. *Proc. Nutr. Soc.* **2014**, *73*, 96–105. [CrossRef] [PubMed]
82. Fichna, J.; Sałaga, M.; Stuart, J.; Saur, D.; Sobczak, M.; Zatorski, H.; Timmermans, J.-P.; Bradshaw, H.B.; Ahn, K.; Storr, M.A. Selective inhibition of FAAH produces antidiarrheal and antinociceptive effect mediated by endocannabinoids and cannabinoid-like fatty acid amides. *Neurogastroenterol. Motil.* **2014**, *26*, 470–481. [CrossRef] [PubMed]
83. Di Marzo, V. New approaches and challenges to targeting the endocannabinoid system. *Nat. Rev. Drug Discov.* **2018**, *17*, 623–639. [CrossRef] [PubMed]
84. Bisogno, T.; Maccarrone, M. Latest advances in the discovery of fatty acid amide hydrolase inhibitors. *Expert Opin. Drug Discov.* **2013**, *8*, 509–522. [CrossRef] [PubMed]

85. Schmidt, H.R.; Kruse, A.C. The Molecular Function of  $\sigma$  Receptors: Past, Present, and Future. *Trends Pharmacol. Sci.* **2019**, *40*, 636–654. [[CrossRef](#)] [[PubMed](#)]
86. Morales-Lázaro, S.L.; González-Ramírez, R.; Rosenbaum, T. Molecular Interplay Between the Sigma-1 Receptor, Steroids, and Ion Channels. *Front. Pharmacol.* **2019**, *10*, 10. [[CrossRef](#)] [[PubMed](#)]
87. Almansa, C.; Vela, J.M. Selective sigma-1 receptor antagonists for the treatment of pain. *Future Med. Chem.* **2014**, *6*, 1179–1199. [[CrossRef](#)] [[PubMed](#)]
88. Kim, F.J.; Kovalyshyn, I.; Burgman, M.; Neilan, C.; Chien, C.-C.; Pasternak, G.W.  $\sigma_1$  Receptor Modulation of G-Protein-Coupled Receptor Signaling: Potentiation of Opioid Transduction Independent from Receptor Binding. *Mol. Pharmacol.* **2010**, *77*, 695–703. [[CrossRef](#)] [[PubMed](#)]
89. Hayashi, T.; Su, T. The Sigma Receptor: Evolution of the Concept in Neuropsychopharmacology. *Curr. Neuropharmacol.* **2005**, *3*, 267–280. [[CrossRef](#)] [[PubMed](#)]
90. Rousseaux, C.G.; Greene, S.F. Sigma receptors [ $\sigma$  Rs]: Biology in normal and diseased states. *J. Recept. Signal Transduct.* **2015**, *36*, 1–62. [[CrossRef](#)] [[PubMed](#)]
91. Ye, N.; Qin, W.; Tian, S.; Xu, Q.; Wold, E.A.; Zhou, J.; Zhen, X.-C. Small Molecules Selectively Targeting Sigma-1 Receptor for the Treatment of Neurological Diseases. *J. Med. Chem.* **2020**, *63*, 15187–15217. [[CrossRef](#)] [[PubMed](#)]
92. Marrazzo, A.; Parenti, C.; Scavo, V.; Ronsisvalle, S.; Maria Scoto, G.; Ronsisvalle, G. In vivo evaluation of (+)-MR200 as a new selective sigma ligand modulating MOP, DOP and KOP supraspinal analgesia. *Life Sci.* **2006**, *78*, 2449–2453. [[CrossRef](#)]
93. Sánchez-Fernández, C.; Nieto, F.R.; González-Cano, R.; Artacho-Cordón, A.; Romero, L.; Montilla-García, Á.; Zamanillo, D.; Baeyens, J.M.; Entrena, J.M.; Cobos, E.J. Potentiation of morphine-induced mechanical antinociception by  $\sigma_1$  receptor inhibition: Role of peripheral  $\sigma_1$  receptors. *Neuropharmacology* **2013**, *70*, 348–358. [[CrossRef](#)]
94. Puente, B.d.l.; Nadal, X.; Portillo-Salido, E.; Sánchez-Arroyos, R.; Ovalle, S.; Palacios, G.; Muro, A.; Romero, L.; Entrena, J.M.; Baeyens, J.M.; et al. Sigma-1 receptors regulate activity-induced spinal sensitization and neuropathic pain after peripheral nerve injury. *Pain* **2009**, *145*, 294–303. [[CrossRef](#)]
95. Romero, L.; Zamanillo, D.; Nadal, X.; Sánchez-Arroyos, R.; Rivera-Arconada, I.; Dordal, A.; Montero, A.; Muro, A.; Bura, A.; Segalés, C.; et al. Pharmacological properties of S1RA, a new sigma-1 receptor antagonist that inhibits neuropathic pain and activity-induced spinal sensitization. *Br. J. Pharmacol.* **2012**, *166*, 2289–2306. [[CrossRef](#)] [[PubMed](#)]
96. Cendán, C.M.; Pujalte, J.M.; Portillo-Salido, E.; Baeyens, J.M. Antinociceptive effects of haloperidol and its metabolites in the formalin test in mice. *Psychopharmacology* **2005**, *182*, 485–493. [[CrossRef](#)]
97. Entrena, J.M.; Cobos, E.J.; Nieto, F.R.; Cendán, C.M.; Baeyens, J.M.; Del Pozo, E. Antagonism by haloperidol and its metabolites of mechanical hypersensitivity induced by intraplantar capsaicin in mice: Role of sigma-1 receptors. *Psychopharmacology* **2009**, *205*, 21–33. [[CrossRef](#)] [[PubMed](#)]
98. Sánchez-Fernández, C.; Entrena, J.M.; Baeyens, J.M.; Cobos, E.J. Sigma-1 Receptor Antagonists: A New Class of Neuromodulatory Analgesics. In *Sigma Receptors: Their Role in Disease and as Therapeutic Agents*; Smith, S., Tsung-Ping, S., Eds.; Springer: Cham, Switzerland, 2017; pp. 109–132.
99. Chien, C.C.; Pasternak, G.W. Selective antagonism of opioid analgesia by a sigma system. *J. Pharmacol. Exp. Ther.* **1994**, *271*, 1583–1590. [[PubMed](#)]
100. Vidal-Torres, A.; de la Puente, B.; Rocasalbas, M.; Touriño, C.; Andreea Bura, S.; Fernández-Pastor, B.; Romero, L.; Codony, X.; Zamanillo, D.; Buschmann, H.; et al. Sigma-1 receptor antagonism as opioid adjuvant strategy: Enhancement of opioid antinociception without increasing adverse effects. *Eur. J. Pharmacol.* **2013**, *711*, 63–72. [[CrossRef](#)] [[PubMed](#)]
101. Zamanillo, D.; Romero, L.; Merlos, M.; Vela, J.M. Sigma 1 receptor: A new therapeutic target for pain. *Eur. J. Pharmacol.* **2013**, *716*, 78–93. [[CrossRef](#)] [[PubMed](#)]
102. Cuevas Cordobes, F.; Almansa-Rosales, C.; Garcia-Lopez, M. Piperidine Derivatives Having Multimodal Activity against Pain. WO2015091939A1, 25 June 2015.
103. Cuevas Cordobes, F.; Almansa-Rosales, C.; Ayet Galcera, E.M.; Serafini Cabanes, M.T.; Garcia-Lopez, M. Piperidine Compounds Having Multimodal Activity Against Pain. WO2015091988A1, 25 June 2015.
104. Cuevas Cordobes, F.; Almansa-Rosales, C.; Garcia-Lopez, M. Piperazine Derivatives Having Multimodal Activity against Pain. WO2015092009A1, 25 June 2015.
105. Prezzavento, O.; Arena, E.; Sánchez-Fernández, C.; Turnaturi, R.; Parenti, C.; Marrazzo, A.; Catalano, R.; Amata, E.; Pasquinucci, L.; Cobos, E.J. (+)- and (–)-Phenazocine enantiomers: Evaluation of their dual opioid agonist/ $\sigma_1$  antagonist properties and antinociceptive effects. *Eur. J. Med. Chem.* **2017**, *125*, 603–610. [[CrossRef](#)] [[PubMed](#)]
106. Lipiński, P.F.J.; Szűcs, E.; Jarończyk, M.; Kosson, P.; Benyhe, S.; Misicka, A.; Dobrowolski, J.C.; Sadlej, J. Affinity of fentanyl and its derivatives for the  $\sigma_1$ -receptor. *Medchemcomm* **2019**, *10*, 1187–1191. [[CrossRef](#)]
107. Largent, B.L.; Wikström, H.; Gundlach, A.L.; Snyder, S.H. Structural determinants of sigma receptor affinity. *Mol. Pharmacol.* **1987**, *32*, 772–784.
108. Chen, J.C.; Smith, E.R.; Cahill, M.; Cohen, R.; Fishman, J.B. The opioid receptor binding of dezocine, morphine, fentanyl, butorphanol and nalbuphine. *Life Sci.* **1993**, *52*, 389–396. [[CrossRef](#)]
109. Lipiński, P.; Kosson, P.; Matalińska, J.; Roszkowski, P.; Czarnocki, Z.; Jarończyk, M.; Misicka, A.; Dobrowolski, J.; Sadlej, J. Fentanyl Family at the Mu-Opioid Receptor: Uniform Assessment of Binding and Computational Analysis. *Molecules* **2019**, *24*, 740. [[CrossRef](#)] [[PubMed](#)]

110. Schmidt, H.R.; Zheng, S.; Gurpinar, E.; Koehl, A.; Manglik, A.; Kruse, A.C. Crystal structure of the human  $\sigma_1$  receptor. *Nature* **2016**, *532*, 527–530. [[CrossRef](#)]
111. García, M.; Virgili, M.; Alonso, M.; Alegret, C.; Fernández, B.; Port, A.; Pascual, R.; Monroy, X.; Vidal-Torres, A.; Serafini, M.-T.; et al. 4-Aryl-1-oxa-4,9-diazaspiro[5.5]undecane Derivatives as Dual  $\mu$ -Opioid Receptor Agonists and  $\sigma_1$  Receptor Antagonists for the Treatment of Pain. *J. Med. Chem.* **2020**, *63*, 2434–2454. [[CrossRef](#)] [[PubMed](#)]
112. García, M.; Virgili, M.; Alonso, M.; Alegret, C.; Farran, J.; Fernández, B.; Bordas, M.; Pascual, R.; Burgueño, J.; Vidal-Torres, A.; et al. Discovery of EST73502, a Dual  $\mu$ -Opioid Receptor Agonist and  $\sigma_1$  Receptor Antagonist Clinical Candidate for the Treatment of Pain. *J. Med. Chem.* **2020**, *63*, 15508–15526. [[CrossRef](#)] [[PubMed](#)]
113. Laggner, C.; Schieferer, C.; Fiechtner, B.; Poles, G.; Hoffmann, R.D.; Glossmann, H.; Langer, T.; Moebius, F.F. Discovery of high-affinity ligands of sigma1 receptor, ERG2, and emopamil binding protein by pharmacophore modeling and virtual screening. *J. Med. Chem.* **2005**, *48*, 4754–4764. [[CrossRef](#)] [[PubMed](#)]
114. Pascual, R.; Almansa, C.; Plata-Salamán, C.; Vela, J.M. A New Pharmacophore Model for the Design of Sigma-1 Ligands Validated on a Large Experimental Dataset. *Front. Pharmacol.* **2019**, *10*, 519. [[CrossRef](#)] [[PubMed](#)]
115. Almansa-Rosales, C.; Garcia-Lopez, M.; Caamano-Moure, A.-M. Spiro-isoquinoline-1,4'-Piperidine Compounds Having Multimodal Activity Against Pain. WO2016078770A1, 26 May 2016.
116. Almansa-Rosales, C. Spiro-Isoquinoline-4,4'-Piperidine Compounds Having Multimodal Activity against Pain. WO2016177472A1, 10 November 2016.
117. Garcia-Lopez, M.; Almansa-Rosales, C. Amide Derivatives Having Multimodal Activity against Pain. WO2017016668A1, 2 February 2017.
118. Torrens-Jover, A.; Jagerovic, N.; Almansa-Rosales, C. Piperidinylalkylamide Derivatives Having Multimodal Activity Against Pain. WO2017178515A1, 19 October 2017.
119. Xiong, J.; Jin, J.; Gao, L.; Hao, C.; Liu, X.; Liu, B.-F.; Chen, Y.; Zhang, G. Piperidine propionamide as a scaffold for potent sigma-1 receptor antagonists and mu opioid receptor agonists for treating neuropathic pain. *Eur. J. Med. Chem.* **2020**, *191*, 112144. [[CrossRef](#)]
120. Xiong, J.; Zhuang, T.; Ma, Y.; Xu, J.; Ye, J.; Ma, R.; Zhang, S.; Liu, X.; Liu, B.-F.; Hao, C.; et al. Optimization of bifunctional piperidinamide derivatives as  $\sigma_1$ R Antagonists/MOR agonists for treating neuropathic pain. *Eur. J. Med. Chem.* **2021**, *226*, 113879. [[CrossRef](#)]
121. Abate, C.; Niso, M.; Berardi, F. Sigma-2 receptor: Past, present and perspectives on multiple therapeutic exploitations. *Future Med. Chem.* **2018**, *10*, 1997–2018. [[CrossRef](#)]
122. Rescifina, A.; Floresta, G.; Marrazzo, A.; Parenti, C.; Prezzavento, O.; Nastasi, G.; Dichiaro, M.; Amata, E. Development of a Sigma-2 Receptor affinity filter through a Monte Carlo based QSAR analysis. *Eur. J. Pharm. Sci.* **2017**, *106*, 94–101. [[CrossRef](#)]
123. Zeng, C.; Mach, R.H. The Evolution of the Sigma-2 ( $\sigma_2$ ) Receptor from Obscure Binding Site to Bona Fide Therapeutic Target. In *Sigma Receptors: Their Role in Disease and as Therapeutic Agents*; Smith, S., Tsung-Ping, S., Eds.; Springer: Cham, Switzerland, 2017; pp. 49–61.
124. Mathia, F.; Marchalín, Š.; Végh, D.; Bobošíková, M.; Halinkovičová, M. Laboratory and industrial synthesis of remifentanyl. *Acta Chim. Slovaca* **2012**, *5*, 145–152. [[CrossRef](#)]
125. Vellemäe, E.; Mastitski, A.; Järv, J.; Veli Hiltunen, J. A Convenient Methanolysis in the Synthesis of Carfentanyl. *Org. Prep. Proced. Int.* **2018**, *50*, 522–526. [[CrossRef](#)]
126. Marton, J.; Glaenzel, B.; Roessler, J.; Golaszewski, D.; Henriksen, G. A Convenient Route to 4-Carboxy-4-Anilidopiperidine Esters and Acids. *Molecules* **2012**, *17*, 2823–2832. [[CrossRef](#)] [[PubMed](#)]
127. Walz, A.J.; Hsu, F.-L. Synthesis of 4-anilino piperidine methyl esters, intermediates in the production of carfentanyl, sufentanyl, and remifentanyl. *Tetrahedron Lett.* **2014**, *55*, 501–502. [[CrossRef](#)]
128. Li, J.; Zhang, T.; Sun, J.; Ren, F.; Jia, H.; Yu, Z.; Cheng, J.; Shi, W. Synthesis and evaluation of peptide-fentanyl analogue conjugates as dual  $\mu/\delta$ -opioid receptor agonists for the treatment of pain. *Chin. Chem. Lett.* **2021**, *in press*. [[CrossRef](#)]
129. Ivanovic, M.; Micovic, I.V.; Vuckovic, S.; Prostran, M.; Todorovic, Z.; Kricojevic, V.D.; Djordjevic, J.B.; Dosen-Micovic, L. The synthesis and preliminary pharmacological evaluation of racemic cis and trans 3-alkylfentanyl analogues. *J. Serbian Chem. Soc.* **2004**, *69*, 511–526. [[CrossRef](#)]
130. Jevtić, I.; Došen-Mičović, L.; Ivanović, E.; Todorović, N.; Ivanović, M. Synthesis of Orthogonally Protected ( $\pm$ )-3-Amino-4-anilidopiperidines and ( $\pm$ )-3-N-Carbomethoxyfentanyl. *Synthesis (Stuttg)* **2017**, *49*, 3126–3136.
131. Mićović, I.V.; Roglič, G.M.; Ivanović, M.D.; Došen-Mičović, L.; Kiricojević, V.D.; Popović, J.B. The synthesis of lactam analogues of fentanyl. *J. Chem. Soc. Perkin Trans.* **1996**, *1*, 2041–2050. [[CrossRef](#)]
132. Congreve, M.; de Graaf, C.; Swain, N.A.; Tate, C.G. Impact of GPCR Structures on Drug Discovery. *Cell* **2020**, *181*, 81–91. [[CrossRef](#)]
133. Lee, Y.; Basith, S.; Choi, S. Recent Advances in Structure-Based Drug Design Targeting Class A G Protein-Coupled Receptors Utilizing Crystal Structures and Computational Simulations. *J. Med. Chem.* **2018**, *61*, 1–46. [[CrossRef](#)]
134. Manglik, A.; Kruse, A.C.; Kobilka, T.S.; Thian, F.S.; Mathiesen, J.M.; Sunahara, R.K.; Pardo, L.; Weis, W.I.; Kobilka, B.K.; Granier, S. Crystal structure of the  $\mu$ -opioid receptor bound to a morphinan antagonist. *Nature* **2012**, *485*, 321–326. [[CrossRef](#)]
135. Huang, W.; Manglik, A.; Venkatakrishnan, A.J.; Laeremans, T.; Feinberg, E.N.; Sanborn, A.L.; Kato, H.E.; Livingston, K.E.; Thorsen, T.S.; Kling, R.C.; et al. Structural insights into  $\mu$ -opioid receptor activation. *Nature* **2015**, *524*, 315–321. [[CrossRef](#)] [[PubMed](#)]

136. Koehl, A.; Hu, H.; Maeda, S.; Zhang, Y.; Qu, Q.; Paggi, J.M.; Latorraca, N.R.; Hilger, D.; Dawson, R.; Matile, H.; et al. Structure of the  $\mu$ -opioid receptor–Gi protein complex. *Nature* **2018**, *558*, 547–552. [[CrossRef](#)] [[PubMed](#)]
137. Lipiński, P.F.J.; Jarończyk, M.; Dobrowolski, J.C.; Sadlej, J. Molecular dynamics of fentanyl bound to  $\mu$ -opioid receptor. *J. Mol. Model.* **2019**, *25*, 144. [[CrossRef](#)]
138. Vo, Q.N.; Mahinthichaichan, P.; Shen, J.; Ellis, C.R. How  $\mu$ -opioid receptor recognizes fentanyl. *Nat. Commun.* **2021**, *12*, 984. [[CrossRef](#)]
139. Mahinthichaichan, P.; Vo, Q.N.; Ellis, C.R.; Shen, J. Kinetics and Mechanism of Fentanyl Dissociation from the  $\mu$ -Opioid Receptor. *JACS Au* **2021**, *1*, 2208–2215. [[CrossRef](#)]
140. Ricarte, A.; Dalton, J.A.R.; Giraldo, J. Structural Assessment of Agonist Efficacy in the  $\mu$ -Opioid Receptor: Morphine and Fentanyl Elicit Different Activation Patterns. *J. Chem. Inf. Model.* **2021**, *61*, 1251–1274. [[CrossRef](#)]
141. Lešnik, S.; Hodošek, M.; Bren, U.; Stein, C.; Bondar, A.-N. Potential Energy Function for Fentanyl-Based Opioid Pain Killers. *J. Chem. Inf. Model.* **2020**, *60*, 3566–3576. [[CrossRef](#)] [[PubMed](#)]
142. Jarończyk, M.; Lipiński, P.F.J.; Dobrowolski, J.C.; Sadlej, J. The FMO analysis of the molecular interaction of fentanyl derivatives with the  $\mu$ -opioid receptor. *Chem. Pap.* **2017**, *71*, 1429–1443. [[CrossRef](#)]
143. Eshleman, A.J.; Nagarajan, S.; Wolfrum, K.M.; Reed, J.F.; Nilsen, A.; Torralva, R.; Janowsky, A. Affinity, potency, efficacy, selectivity, and molecular modeling of substituted fentanyls at opioid receptors. *Biochem. Pharmacol.* **2020**, *182*, 114293. [[CrossRef](#)] [[PubMed](#)]
144. Wu, Z.; Hruby, V.J. Toward a Universal  $\mu$ -Agonist Template for Template-Based Alignment Modeling of Opioid Ligands. *ACS Omega* **2019**, *4*, 17457–17476. [[CrossRef](#)] [[PubMed](#)]
145. Kooistra, A.J.; Mordalski, S.; Pándy-Szekeres, G.; Esguerra, M.; Mamyrbekov, A.; Munk, C.; Keserű, G.M.; Gloriam, D.E. GPCRdb in 2021: Integrating GPCR sequence, structure and function. *Nucleic Acids Res.* **2021**, *49*, D335–D343. [[CrossRef](#)] [[PubMed](#)]
146. Schmidt, H.R.; Betz, R.M.; Dror, R.O.; Kruse, A.C. Structural basis for  $\sigma_1$  receptor ligand recognition. *Nat. Struct. Mol. Biol.* **2018**, *25*, 981–987. [[CrossRef](#)] [[PubMed](#)]
147. Alon, A.; Lyu, J.; Braz, J.M.; Tummino, T.A.; Craik, V.; O’Meara, M.J.; Webb, C.M.; Radchenko, D.S.; Moroz, Y.S.; Huang, X.-P.; et al. Structures of the  $\sigma_2$  receptor enable docking for bioactive ligand discovery. *Nature* **2021**, *600*, 759–764. [[CrossRef](#)] [[PubMed](#)]
148. Yin, J.; Chapman, K.; Clark, L.D.; Shao, Z.; Borek, D.; Xu, Q.; Wang, J.; Rosenbaum, D.M. Crystal structure of the human NK 1 tachykinin receptor. *Proc. Natl. Acad. Sci. USA* **2018**, *115*, 13264–13269. [[CrossRef](#)]
149. Schöppe, J.; Ehrenmann, J.; Klenk, C.; Rucktooa, P.; Schütz, M.; Doré, A.S.; Plückthun, A. Crystal structures of the human neurokinin 1 receptor in complex with clinically used antagonists. *Nat. Commun.* **2019**, *10*, 17. [[CrossRef](#)]
150. Chen, S.; Lu, M.; Liu, D.; Yang, L.; Yi, C.; Ma, L.; Zhang, H.; Liu, Q.; Frimurer, T.M.; Wang, M.-W.; et al. Human substance P receptor binding mode of the antagonist drug aprepitant by NMR and crystallography. *Nat. Commun.* **2019**, *10*, 638. [[CrossRef](#)] [[PubMed](#)]
151. Thom, C.; Ehrenmann, J.; Vacca, S.; Waltenspühl, Y.; Schöppe, J.; Medalia, O.; Plückthun, A. Structures of neurokinin 1 receptor in complex with G q and G s proteins reveal substance P binding mode and unique activation features. *Sci. Adv.* **2021**, *7*, eabk2872. [[CrossRef](#)] [[PubMed](#)]
152. Harris, J.A.; Faust, B.; Gondin, A.B.; Dämgen, M.A.; Suomivuori, C.-M.; Veldhuis, N.A.; Cheng, Y.; Dror, R.O.; Thal, D.M.; Manglik, A. Selective G protein signaling driven by substance P–neurokinin receptor dynamics. *Nat. Chem. Biol.* **2022**, *18*, 109–115. [[CrossRef](#)] [[PubMed](#)]
153. Wang, S.; Wacker, D.; Levit, A.; Che, T.; Betz, R.M.; McCorvy, J.D.; Venkatakrishnan, A.J.; Huang, X.-P.; Dror, R.O.; Shoichet, B.K.; et al. D 4 dopamine receptor high-resolution structures enable the discovery of selective agonists. *Science* **2017**, *358*, 381–386. [[CrossRef](#)] [[PubMed](#)]
154. Zhou, Y.; Cao, C.; He, L.; Wang, X.; Zhang, X.C. Crystal structure of dopamine receptor D4 bound to the subtype selective ligand, L745870. *Elife* **2019**, *8*, e48822. [[CrossRef](#)] [[PubMed](#)]
155. Chien, E.Y.T.; Liu, W.; Zhao, Q.; Katritch, V.; Won Han, G.; Hanson, M.A.; Shi, L.; Newman, A.H.; Javitch, J.A.; Cherezov, V.; et al. Structure of the Human Dopamine D3 Receptor in Complex with a D2/D3 Selective Antagonist. *Science* **2010**, *330*, 1091–1095. [[CrossRef](#)] [[PubMed](#)]
156. Xu, P.; Huang, S.; Mao, C.; Krumm, B.E.; Zhou, X.E.; Tan, Y.; Huang, X.-P.; Liu, Y.; Shen, D.-D.; Jiang, Y.; et al. Structures of the human dopamine D3 receptor–Gi complexes. *Mol. Cell* **2021**, *81*, 1147–1159.e4. [[CrossRef](#)] [[PubMed](#)]
157. Wang, S.; Che, T.; Levit, A.; Shoichet, B.K.; Wacker, D.; Roth, B.L. Structure of the D2 dopamine receptor bound to the atypical antipsychotic drug risperidone. *Nature* **2018**, *555*, 269–273. [[CrossRef](#)] [[PubMed](#)]
158. Fan, L.; Tan, L.; Chen, Z.; Qi, J.; Nie, F.; Luo, Z.; Cheng, J.; Wang, S. Haloperidol bound D2 dopamine receptor structure inspired the discovery of subtype selective ligands. *Nat. Commun.* **2020**, *11*, 1074. [[CrossRef](#)]
159. Yin, J.; Chen, K.-Y.M.; Clark, M.J.; Hijazi, M.; Kumari, P.; Bai, X.; Sunahara, R.K.; Barth, P.; Rosenbaum, D.M. Structure of a D2 dopamine receptor–G-protein complex in a lipid membrane. *Nature* **2020**, *584*, 125–129. [[CrossRef](#)] [[PubMed](#)]
160. Im, D.; Inoue, A.; Fujiwara, T.; Nakane, T.; Yamanaka, Y.; Uemura, T.; Mori, C.; Shiimura, Y.; Kimura, K.T.; Asada, H.; et al. Structure of the dopamine D2 receptor in complex with the antipsychotic drug spiperone. *Nat. Commun.* **2020**, *11*, 6442. [[CrossRef](#)] [[PubMed](#)]
161. Zhuang, Y.; Xu, P.; Mao, C.; Wang, L.; Krumm, B.; Zhou, X.E.; Huang, S.; Liu, H.; Cheng, X.; Huang, X.-P.; et al. Structural insights into the human D1 and D2 dopamine receptor signaling complexes. *Cell* **2021**, *184*, 931–942.e18. [[CrossRef](#)]

162. Hua, T.; Vemuri, K.; Pu, M.; Qu, L.; Han, G.W.; Wu, Y.; Zhao, S.; Shui, W.; Li, S.; Korde, A.; et al. Crystal Structure of the Human Cannabinoid Receptor CB1. *Cell* **2016**, *167*, 750–762.e14. [[CrossRef](#)] [[PubMed](#)]
163. Shao, Z.; Yin, J.; Chapman, K.; Grzemska, M.; Clark, L.; Wang, J.; Rosenbaum, D.M. High-resolution crystal structure of the human CB1 cannabinoid receptor. *Nature* **2016**, *540*, 602–606. [[CrossRef](#)] [[PubMed](#)]
164. Hua, T.; Vemuri, K.; Nikas, S.P.; Laprairie, R.B.; Wu, Y.; Qu, L.; Pu, M.; Korde, A.; Jiang, S.; Ho, J.-H.; et al. Crystal structures of agonist-bound human cannabinoid receptor CB1. *Nature* **2017**, *547*, 468–471. [[CrossRef](#)] [[PubMed](#)]
165. Hua, T.; Li, X.; Wu, L.; Iliopoulos-Tsoutsouvas, C.; Wang, Y.; Wu, M.; Shen, L.; Brust, C.A.; Nikas, S.P.; Song, F.; et al. Activation and Signaling Mechanism Revealed by Cannabinoid Receptor-Gi Complex Structures. *Cell* **2020**, *180*, 655–665.e18. [[CrossRef](#)]
166. Shao, Z.; Yan, W.; Chapman, K.; Ramesh, K.; Ferrell, A.J.; Yin, J.; Wang, X.; Xu, Q.; Rosenbaum, D.M. Structure of an allosteric modulator bound to the CB1 cannabinoid receptor. *Nat. Chem. Biol.* **2019**, *15*, 1199–1205. [[CrossRef](#)] [[PubMed](#)]
167. Krishna Kumar, K.; Shalev-Benami, M.; Robertson, M.J.; Hu, H.; Banister, S.D.; Hollingsworth, S.A.; Latorraca, N.R.; Kato, H.E.; Hilger, D.; Maeda, S.; et al. Structure of a Signaling Cannabinoid Receptor 1-G Protein Complex. *Cell* **2019**, *176*, 448–458.e12. [[CrossRef](#)] [[PubMed](#)]
168. Wang, X.; Liu, D.; Shen, L.; Li, F.; Li, Y.; Yang, L.; Xu, T.; Tao, H.; Yao, D.; Wu, L.; et al. A Genetically Encoded F-19 NMR Probe Reveals the Allosteric Modulation Mechanism of Cannabinoid Receptor 1. *J. Am. Chem. Soc.* **2021**, *143*, 16320–16325. [[CrossRef](#)]